iAtlantic Deliverable D2.1:

Basin-wide Atlantic marine landscape map

Project acronym:	iAtlantic
Grant agreement number:	818123
Deliverable number:	D2.1
Deliverable title:	Basin-wide Atlantic marine landscape map
Work package:	WP2
Date of completion:	24/09/2021
Authors:	Mia Schumacher, Dr. Veerle Huvenne, Prof. Dr. Colin Devey, Prof. Dr. Pedro Martínez Arbizu, Prof. Dr. Arne Biastoch, Stefan Meinecke

This project has received funding from the European Union's Horizon 2020 research and innovation programme under grant agreement No 818123 (iAtlantic). This output reflects only the author's view and the European Union cannot be held responsible for any use that may be made of the information contained therein.

Table of Contents

Abstract

Classifications of the marine environment give a comprehensive and unpretentious overview into regions of similar characteristics and can hence be a stepping stone for sustainable ocean resource handling and protection plans. There have been many efforts to categorise the marine realm into seascapes or hydro-morphologic provinces, using different approaches, applied at a wide range of scales. Some of those categorisations available are based on hierarchical classification schemes with often arbitrary thresholds or use simple algorithms which do not fully account for the high complexity of the data. This study presents a basin-wide classification of the Atlantic seafloor environment, based on nine global datasets: bathymetry, slope, terrain ruggedness index, topographic position index, sediment thickness, POC flux, salinity, dissolved oxygen, temperature, current velocity and phytoplankton. To reduce subjectivity within the analysis, an unsupervised classification was performed on the normalised data using Gaussian finite mixture models. Those models describe a latent distribution structure of the input data set from which the final clusters, here seabed areas (SBAs), are derived. This model-based clustering approach seeks to overcome the shortcomings of other classification techniques by trying to embrace the challenging complexity of the ocean floor environment.

The result is a map of the Atlantic realm subdivided into nine SBAs. Some are clearly defined by geological and geomorphological properties, while others are dominated by hydrographic properties, or by a mixture of both sea floor terrain and water column characteristics. Larger SBAs cover the deep abyssal plain with low hydrographic and seasonal variation – in contrast to smaller SBAs including coastal waters that are subject to high seasonal variability. There are also differences in geographical distributions. The SBAs we found were further compared to other existing classifications (e.g., Global Ocean Seascapes, GOODS, EMU) and supplementary data (e.g., seamount locations) to assess in how far the objectively identified SBAs are represented in former classifications and studies.

1. Introduction

This study presents a classification of the Atlantic seafloor environment based on selected geomorphological and oceanographic parameters.

1.1 Marine landscape classifications

The ocean environment is perceived as vast and seemingly endless variable, and so are its inhabitants. It may be argued that breaking it down into a handful of distinct classes does not account for its diversity. However, if we aim to develop sustainable practices, particularly grounded in ecosystem-based management (typically using area-based management tools, (e.g., IUCN, 2018)), there is a need to comprise this variability in spatially explicit delineations of biological and environmental entities. As such, there is a need to classify the marine ecosystem into 'provinces', 'landscapes' or 'habitats' (Roff et al., 2003). Indeed, Kavanaugh et al. (2016) summarise that, 'landscapes are conceptual models of systems shaped by the local geomorphology, environmental conditions and biological processes.'

A variety of different classifications have been developed for the global ocean, based on a wide range of approaches. Most of these either start from a biological point of view, leaning on the knowledge of species distributions and leading to the delineation of biomes or biogeographic provinces (e.g., Watling et al., 2013), or from the physiographic point of view, deploying a classification of the physical environment as a proxy for species niches and habitats (e.g., Harris et al., 2014). Unfortunately, due to the remoteness and challenging sampling conditions in the deep and open ocean, our knowledge of species distributions in the marine realm is still very limited, creating considerable uncertainties in biogeographic classifications of the ocean (even despite the significant progress in this realm by large research programmes such as the Census of Marine Life) (Snelgrove, 2010). Predictions of the distribution patterns of species and biomass

are typically made using physical environmental variables as predicting factors, given the fact that, particularly at broad scales, the physical environment is one of the main drivers for species occurrence and community composition, and is commonly better known or observed (Morato et al., 2021; Gille et al., 2004; Wei et al., 2010; Watling, 2013). This means that the large-scale ecosystem classifications of the oceans[1] typically start with broad divisions of the physical environment, based on key parameters that influence species' physiology, distribution and behaviour (e.g., depth, temperature, oxygen concentration, and food availability). A robust classification of the marine environment into its physiographic entities therefore provides a first-level insight into the spatial structure of ocean ecosystems and can serve as a tool to indicate ecosystem connectivity or patchiness, as well as support marine protected area networks assessments (Popova et al., 2019) or other aspects of marine spatial planning and conservation (Combes et al., 2021).

Although the sea floor and the water mass above it are not two entirely independent ecosystems, the driving factors influencing those regimes still significantly differ from one another (Roff, 2003; Harris and Whiteway, 2009). Due to topography acting as a barrier for many benthic and demersal species (Morato et al., 2021), life on the sea floor is less interconnected and dynamic compared to the pelagic, and benthic habitats tend to be more stable over time (UNESCO, 2009). In this study, we focus on the sea floor of the Atlantic Ocean which strongly determines our input data selection. Other studies have focussed on pelagic/water column classification (e.g., Kavanaugh et al. 2016; Sonnewald et al., 2020), some of them focussed on the North Atlantic (EUNIS; Davies et al., 2004). A good but by no means exhaustive review about existing classifications is given by Howell (2010).

1.2 Need for objectivity

Since there are already multiple classifications of the global ocean, an important question is, 'why do we need yet another?' The answer is that there is a need for enhanced objectivity. With this study, we aim to reduce human subjectivity as far as possible by avoiding setting a priori thresholds between classes and applying a multivariate statistical approach. Thresholds that are based on human interpretation of what exists on the sea floor bear the risk of overlooking specific types of marine landscapes by considering only a few aspects of the environment each time and may introduce artificial divisions because of the way that people historically looked at ocean maps and biological data (Howell, 2010). In reality, the physical environment is a multivariate continuum. Ideally, all aspects of its character should be considered simultaneously when delineating significantly different environmental entities or landscapes. Multivariate data analysis techniques are capable of this, and can take marine landscape classification beyond the initial, manual approach (Kavanaugh et al. 2016). To date and to our knowledge, only two studies exist, the Global Seascapes by Harris & Whiteway (2009) and the Environmental Marine Units (EMU) by Sayre et al. (2019), which aim to take an objective approach using unsupervised classification techniques on datasets that include hydrographic, morphological and biological variables on a global scope.

Applying a fully unsupervised machine learning algorithm, we aim to explore the potential differences to the existing hierarchical classifications, identifying any types of seafloor environments that are easily overlooked. Unsupervised (in contrast to supervised) in this sense means that the clustering procedure is an automatic process, recognising patterns in an unlabelled data set. This kind of multivariate statistical clustering schemes treat all input determinants equally. Ultimately, we will use our classification results to refine and update the Atlantic section of the Global seascape map by Harris and Whiteway (2009) (*Figure 1*). These authors applied an unsupervised isoclass technique, which is comparable to a step-wise (cascaded) K-Means, on six biophysical variables (i.e., depth, seabed slope, sediment thickness, primary production, bottom water dissolved oxygen, and bottom temperature).

[1] E.g., European Nature Information System (hereafter EUNIS) by Davies et al., 2004; Global Seascape Map by Harris and Whiteway, 2009; Global Open Ocean and Deep Seabed (hereafter GOODS) biogeographic classification by the United Nations Educational, Scientific and Cultural Organization (hereafter UNESCO), 2009; Global Seafloor Features Map (hereafter GSFM) by Harris et al., 2014, Environmental Marine Units (hereafter EMU) by Sayre et al., 2017.

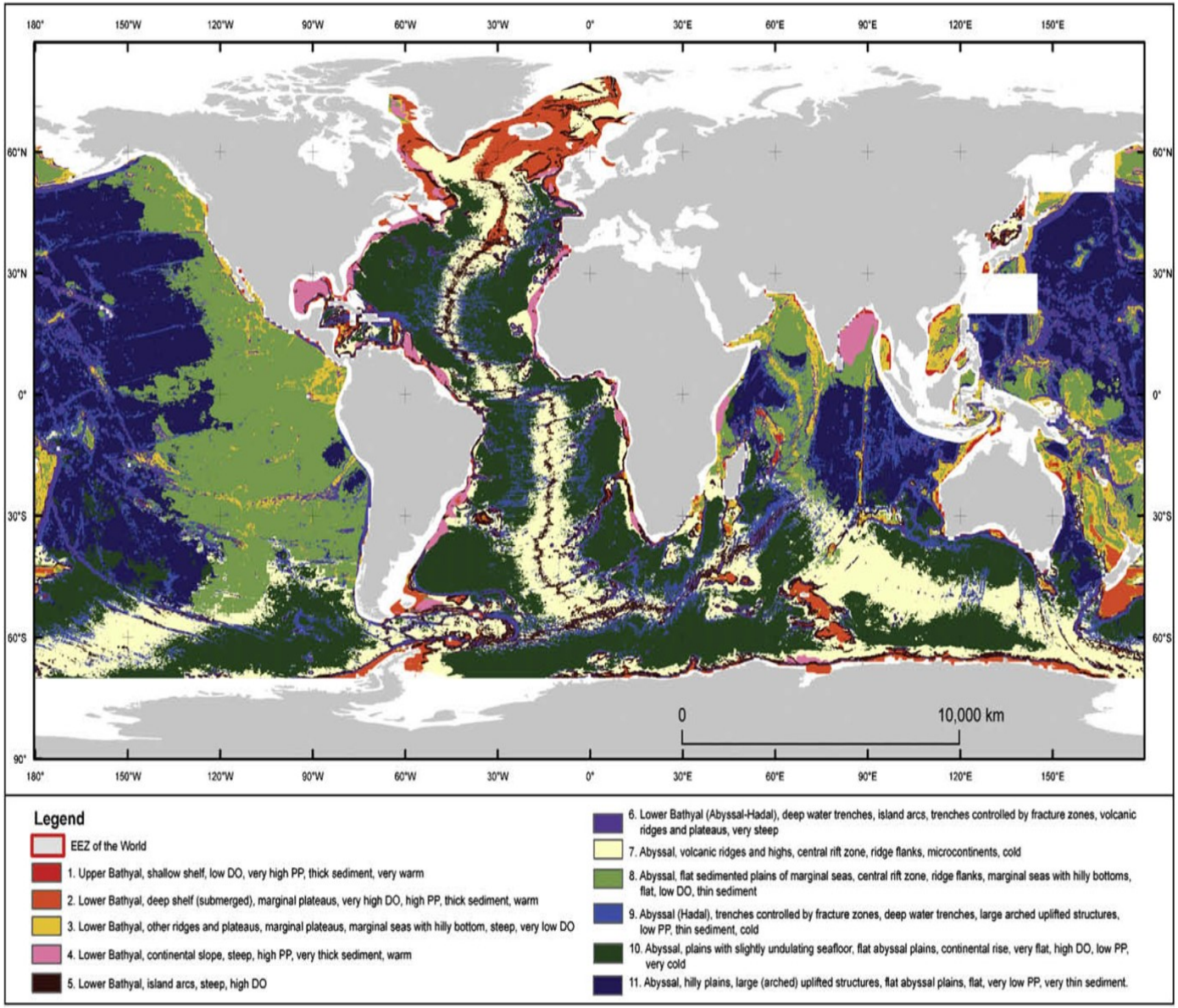

Figure 1: Global Seascape Map by Harris and Whiteway (2009)

Within our study, we aim to expand the range of input determinants, including latest data from recent and fine-scaled processed ocean models. Using density estimation and model-based clustering, we try to overcome shortcomings of the widely used K-Means, or of similar algorithms (e.g. isoclass), such as their sensitivity of initial cluster centre placement, fixed number of clusters, limitation to spherically shaped clusters, etc. (Press et al., 2007; Sayre et al., 2019).

We believe that this describes the ocean environment in a holistic way, which is closer to reality. At the same time, we acknowledge that the resolution of data on the seafloor is still low, especially in the open ocean where in-situ samples are scarce. Therefore, even the most complex technique inherits a large uncertainty. We termed the clusters as identified by the clustering algorithm 'seabed areas (SBAs)'. In the following sections, both of those expressions, clusters and SBAs, will be used as synonyms.

2. Methods-Processing Steps

We applied a density estimation and model-based clustering technique implemented by (finite) Gaussian mixture models (GMM). This technique reveals latent structures within the data set by seeking an optimal number of Gaussian distributions that sufficiently represent the data set. Those distributions or models are fitted iteratively by the maximum-likelihood estimation algorithm 'Expectation Maximisation' (EM): For each point of the data set, the probability of belonging to a model (cluster) is estimated (expectation, E-step) using each Gaussian's current mean, its covariance matrix and a hidden mixing probability coefficient as fitting parameters. The expectation step is then repeated (maximisation, M-step) until convergence (stabilisation of the model) (Scrucca and Raftery, 2014). The optimum model (= best number of clusters) is selected by the Bayesian Information Criterion (BIC) index which is known to be robust against overfitting (Press et al., 2007). The E-M-step is somewhat analogue to calculating the distance of each point to the cluster centre for a data point in KMeans. In fact, KMeans is a special, simplified case of GMM (Press et al., 2007). GMM however has the following advantage over KMeans: the number of clusters does not have to be known à priori. Furthermore, GMM accepts clusters of various shape, volume and orientation and is not sensitive to the initial placement of cluster centres. Given that it is based on probability, the cluster boundaries are not hard (i.e. either a point belongs to a cluster or not) but soft, meaning that there is a certain probability that a data point is part of a cluster.

To assess whether to include or exclude variables as input parameters, a variable selection algorithm is run before the actual clustering. It examines the differences of BIC indices depending on whether a variable has clustering properties or not. Based on this, a variable is accepted or rejected. A large positive BIC difference indicates high clustering properties (Scrucca and Raftery, 2014). The algorithm accepted all input variables as input parameters.

2.1. Data Selection

Deciding on the right input parameters for the classification is a fundamental but also a challenging task. In an unsupervised cluster analysis, it is this part which can mostly be influenced by human subjectivity, with incorrect choices at this stage potentially rendering biased results (Roff et al., 2003; Harris and Whiteway, 2009). We selected data based on the following: ecological understanding described in the literature and existing classifications (e.g., Harris and Whiteway, 2009; Gille et al. 2009; Howell, 2010; Watling et al., 2013; Harris et al., 2014; Sayre et al. 2019; Morato et al. 2021), spatial coverage, resolution, data access, and data format to have an expressive sample of ecological determinants and a good representation of the sea floor ecosystem. In our aim to map hydro-morphological provinces of the Atlantic seafloor, the spatial availability of input data was constrained to the iAtlantic geographical boundary and further excluded data from the sea surface and the water column (except for the bottom water). For example, in the deep sea, where data presence is scarce and the major area to be classified is below -1,000m, we relied on models and data compilations that are available in full coverage and not in

single scattered sample points. For the sake of data integrity and homogeneity, we tried to reduce the number of different data sources, which led us to choose the Copernicus Mercator model (hereafter CMEMS) (EU Copernicus Marine Service, 2021) for the hydrographic variables and the Satellite Radar Topography Mission version 2 (hereafter SRTM) 15+V2 data (Tozer et al., 2019a) for the geomorphological parameters. CMEMS provides the most accurate and regularly updated information by combining ocean models with in-situ and remotely sensed data into one publicly available product. The SRTM15+ V2 grid was taken as topographical input into the analysis. Furthermore, GlobSed (Updated Total Sediment Thickness in the World's Oceans, Straume et al. 2019) and Particulate Organic Carbon (POC) flux (Lutz 2007) have been chosen as classification parameters. All data are unprojected and are referenced to World Geodetic System (WGS) 84.

2.2 Data Acquisition and Description

2.2.1. CMEMS Data Products

The CMEMS is the marine part of the EU Earth observation programme Copernicus that was launched in 1998 by the European Commission and the European Space Agency (ESA). Global physical and biochemical data from satellite observations, ocean models and in-situ samples are combined and published on a regular basis, and provide information on the physical and biochemical state, dynamics, and variability of the ocean ecosystem. All data products are freely available to the public (EU Copernicus Marine Service, 2021).

The data used for this study are based on numerical models (NEMO 3.1, ORCA12) and data assimilation techniques (reduced order Kalman filter) (Lellouche et al., 2018). The following parameters were extracted:

- Bottom temperature in [°C] (physical), resolution 1/12°
- Salinity in [psu] (physical), resolution 1/12°
- East (UO) and north current velocity (VO) components in [m/s] (physical), resolution 1/12°
- Oxygen in [mmol/m^3] (biochemical), resolution ¼ °
- Phytoplankton in [mol] (biochemical) expressed as carbon in sea water, resolution ¼ °

The CMEMS provides all hydrographic data products via FTP server download as global multiband and multi - dimensional NetCDF files. The dimensions are: Time, latitude, longitude, depth (50 layers), and 11 value variables (salinity, oxygen, etc.).

The physical data product (GLOBAL_ANALYSIS_FORECAST_PHY_001_024_monthly) is based on the PSY4V3 Mercator system of the NEMO 3.1 model and contains 3D monthly mean fields for temperature, salinity, and current velocity amongst others. These data come with a horizontal resolution of 1/12° (approximately 8 km at the equator) with 50 depth levels and a vertical resolution of 1 m at the sea surface and 450 m at the sea floor depth level (Lellouche et al., 2018; Tressol et al., 2020).

The biochemical data products (GLOBAL_ANALYSIS_FORECAST_BIO_001_028) are based on the PISCES-v2 (Pelagic Interactions Scheme for Carbon and Ecosystem Studies volume 2) model within NEMO 3.6 which simulates biochemical and lower trophic levels of marine ecosystems, as well as carbon and main nutrient cycles (Aumont et al., 2015). It also contains 3D monthly mean fields for oxygen and phytoplankton and comes with a horizontal resolution of ¼° (approximately 24 km at the equator). Similar to the physical data, it has 50 depth levels at a vertical resolution of 1 m on the sea surface and 450 m at the sea floor depth level (Paul, 2019).

In summary, the selected hydrographic data have been reduced to sea floor level (i.e., CMEMS depth layers closest to sea floor), averaged over the last three years (2018 - 2020) and, additionally, three years' seasonal variability was calculated. An overview of all input variables and their main statistics is listed in

the appendix (*Appendix*). A detailed description of the data preparation and processing is given below.

2.2.2 SRTM15+ V2

The latest Shuttle Radar Topography Mission (SRTM) version 2 digital topographic dataset released by NASA in 2015 is the basis to the topography determinant in our classification. Satellite altimetry measures the Earth's gravity field to estimate topography. Water depth, hence sea floor bathymetry, can be predicted by sea surface slope measurements. Depending on the satellites' track spacing, latitude, and water depth, the resolution of the predicted bathymetry is approximately 6 km (Tozer et al., 2019a).

The SRTM15+ V2 grid is available via OpenTopography (https://opentopography.org/) as a global NetDCF. It is a data compilation made by Tozer et al. (2019a) of the SRTM predicted ocean depth complemented by shipborne MBES bathymetry at 15" (1/240°) resolution. To avoid bias towards higher resolution data during the classification, the SRTM15+ V2 has been down-sampled to the CMEMS data product resolution of 1/12° (Yesson et al., 2011a, b). The following variables were used from Tozer et al. (2019b):

- Terrain ruggedness index TRI, resolution 1/240°, rescaled to 1/12°
- Topographic position index TPI, resolution 1/240°, rescaled to 1/12°
- Slope in [°], resolution 1/240°, rescaled to 1/12°
- Depth in [m] , resolution 1/240°, rescaled to 1/12°

2.2.3 Global Sediment Layer Thickness and POC flux

The latest compilation for sediment thickness data GlobSed (Straume et al. 2019) was used as sedimentation is a crucial indicator for ecosystem types and biodiversity (e.g., Snelgrove, 1999; Zeppili et al. 2016). It was also used as a proxy for the sedimentation rate since there is currently no Atlantic-wide full-coverage dataset that reflects sedimentation rate across the basin. GlobSed is the most updated version of global sedimentation information and has been constructed at the same resolution as the CMEMS data. Particulate Organic Carbon (POC) flux (Lutz, 2007) has further been chosen as a proxy for food availability at the sea floor in addition to phytoplankton (from CMEMS) (e.g. Kharbush et al., 2020; Kirsty et al. 2020). Hence, the two last classification parameters were added:

- Sediment layer thickness in [m], resolution 1/12°
- POC flux, resolution 1/11°, rescaled to 1/12°

2.3 Data Pre-Processing

The processing has been done using gdal (GDAL/OGR 2021), Python V3.7 (Van Rossum & Drake 2009) and GMT Generic mapping Tools V6.1.1 (Wessel et al., 2019) in a jupyter notebook. Data were visualised with QGIS V3.16 (Hannover) (QGIS Development Team 2020). The pre-processing steps are explained below.

2.3.1 Data Pre-Processing Oceanography

a. Reduction of dimension I: The variables chosen as input were extracted for the classification from the multidimensional NetCDF and save as Geotiff, using gdal_translate. This had to be performed on each of the selected input variables separately. Considering that the NetCDFs were monthly products, the number of the output files was 5x3x12 Geotiffs, each containing 50 depth layers for each parameter (i.e., bottom temperature, salinity, north- and east current velocity, oxygen, phytoplankton) per month of the three-year period from 2018 to 2020 (36 months in total).

b. Reduction of dimension II: The depth layers from the files created in step 1 for all parameters and months were split into single Geotiffs to create a sea floor layer. This was done using gdal_translate. The output file contains one parameter at one depth (D1 – D50) for each month. In total, these were 50x5x3x12 Geotiffs for all input parameters and 36 months. Note that the bottom temperature was already at seafloor level and, hence, this processing step was skipped for that variable.
c. Some of the data required scaling, as stated by CMEMS: The scaling factors can either be looked up in the respective data product manual or be derived using gdalinfo on the files. The scaling was applied where necessary using gdal_calc.py. This was true for salinity, bottom temperature, and the current velocities.
d. Create a bottom layer for all parameters: All depth layers were merged on top of each other in the right order (from the sea surface D1 to the sea floor level D50) so that the values of the next deeper depth layer would replace the previous pixel values, unless their value was NaN. The output was one file containing sea floor layers: D1 + D2 + … + D50 (one tiff per month containing one parameter as sea floor depth level). Note that this processing step was based on the CMEMS depth zonation which was very coarsely terraced - from steps of several meters at the sea surface towards steps of several hundreds of meters in the deep water (Lellouche et al., 2019). Thus, this was not strictly a sea floor layer; it was rather the deepest layer available from CMEMS. It will still be referred to as such in the following sections, as these are currently the best data available. Furthermore, we assumed that the depth related variation of the input parameters was low in deep water and the deepest-layer approach was a good approximation to the conditions prevailing at the sea floor. The output was one bottom layer Geotiff per month per input variable, in total 5x3x12.
e. For O_2 and phytoplankton only: These layers needed to be up-scaled due to resolution differences between the biology (1/4°) and the physical (1/12°) data products. This was done with the grdsample algorithm in Generic Mapping Tools (GMT) (Wessel et al.; 2019) using a bilinear interpolation with a threshold of 0.5 for NaNs.

2.3.2 Data Pre-Processing Morphology

a. To avoid unforeseeable bias and interpolation effects towards higher resolution data, which is likely to occur when upscaling over a wide resolution range, the SRTM15+ V2 (1/240°) has been down sampled to CMEMS resolution (1/12°). The resampling was done with the GMT grdsample algorithm.
b. Three bathymetry derivatives were calculated using gdal_dem: Topographic position index (TPI), Terrain ruggedness index (TRI), and slope. For TPI and TRI, a 3x3 pixel neighbourhood was applied as search radius. This was thought to be a sensible scale to include prominent features without the risk of distorting the result by putting the emphasis on small features. Dimensioning TPI is highly scale-dependent and strongly related to slope. It is positive at elevations, negative in depressions, and near zero in flat areas. TPI description was based on Weiss (2001) and associated with slope measures. Denotation for TRI levels was adopted from Riley et al. (1999). Considering the resolution of 1/12°, TPI, TRI and slope smooth out features smaller than this.
c. The POC flux grid (Lutz et al., 2007) was resampled to a resolution of 1/12° using GMT grdsample algorithm.

2.3.4 All Data

a. The current velocity data sets, as well as the GlobSed sediment thickness grid, occasionally lacked data values, especially near the sea floor. To avoid unnecessary data gaps in the classification, those gaps were filled using GMT grdfill with the nearest neighboring algorithm, as the data holes only affected very few isolated cells.

b. Landmasses have been 'stamped' out (i.e., land areas were filled with NaNs) with the landmask as provided by CMEMS using gdal_calc.py. To ensure uniform NaN values for all input variables, this has been done for all layers simultaneously. The area covered was then restricted to the iAtlantic geographic boundary.

2.4 Data Processing

a. All of the pre-processed Geotiffs (5x3x12 + 5 = 180 files in total) were opened with python and converted to numpy arrays.
b. From the partial current velocity components uo and vo, the absolute current velocity was calculated: $v = sqrt(uo^2 + vo^2)$. The absolute velocity was adopted as a new input parameter instead of the velocity components.
c. For each of temperature, salinity, current velocity, oxygen and phytoplankton, a three-year annual mean: [((Jan18 + Jan19 + Jan20) + (Feb18 +)… + (Dec20))/36] along with a three-year seasonal variability |summer – winter|(where: Summer = (June + July + Aug.)/3 and Winter = (Dec. + Jan. + Feb.)/3) were calculated.
d. The calculated annual and seasonal means of the hydrographic data along with the bathymetry, its derivatives, sediment thickness and POC flux were exported into a comma separated text file (.csv), containing 18 columns and 1,810,748 rows. A summary of the statistics is listed in the appendix (*Table 2* and *Table 3*). This file served as input for the classification. It will be referred to as IPF hereafter.
e. For easier handling later on in the classification process, all lines in the IPF containing NaN values (i.e., landmass) were removed.

2.5 Data Classification

The clustering was performed using R V4.1 (R core team 2018):

a. The IPF was opened in R and scaled to avoid bias towards extreme values and obtain zero mean and unit variance.
b. A variable selection algorithm ('clustvarsel') was applied on the IPF to identify the optimal subset of input parameters, based on their clustering properties (Scrucca and Raftery, 2018). According to its result, all variables have been accepted as clustering input.
c. The Gaussian mixture modelling algorithm 'mclust' (Scrucca et al., 2016) was applied on the entire input variable data set.
d. Boxplots were created using 'ggplot2' (Whickham, 2016) and the 'RcolourBrewer' (Brewer, 2013) library.

3. Results and Interpretation

3.1 Overview

Figure 2 shows the map of the Atlantic sea floor and the identified SBAs as a result of the classification. We found nine SBAs in total that are well distinguishable and explainable. The majority of SBA is located in the deep, open ocean in Areas beyond national jurisdiction, ABNJs, whereas only two SBAs were coast-adjacent and continental shelf regions.

Table 1 gives an overview of the SBAs along with a short description and the total area covered. In the following sections, the SBAs will be described in more detail.

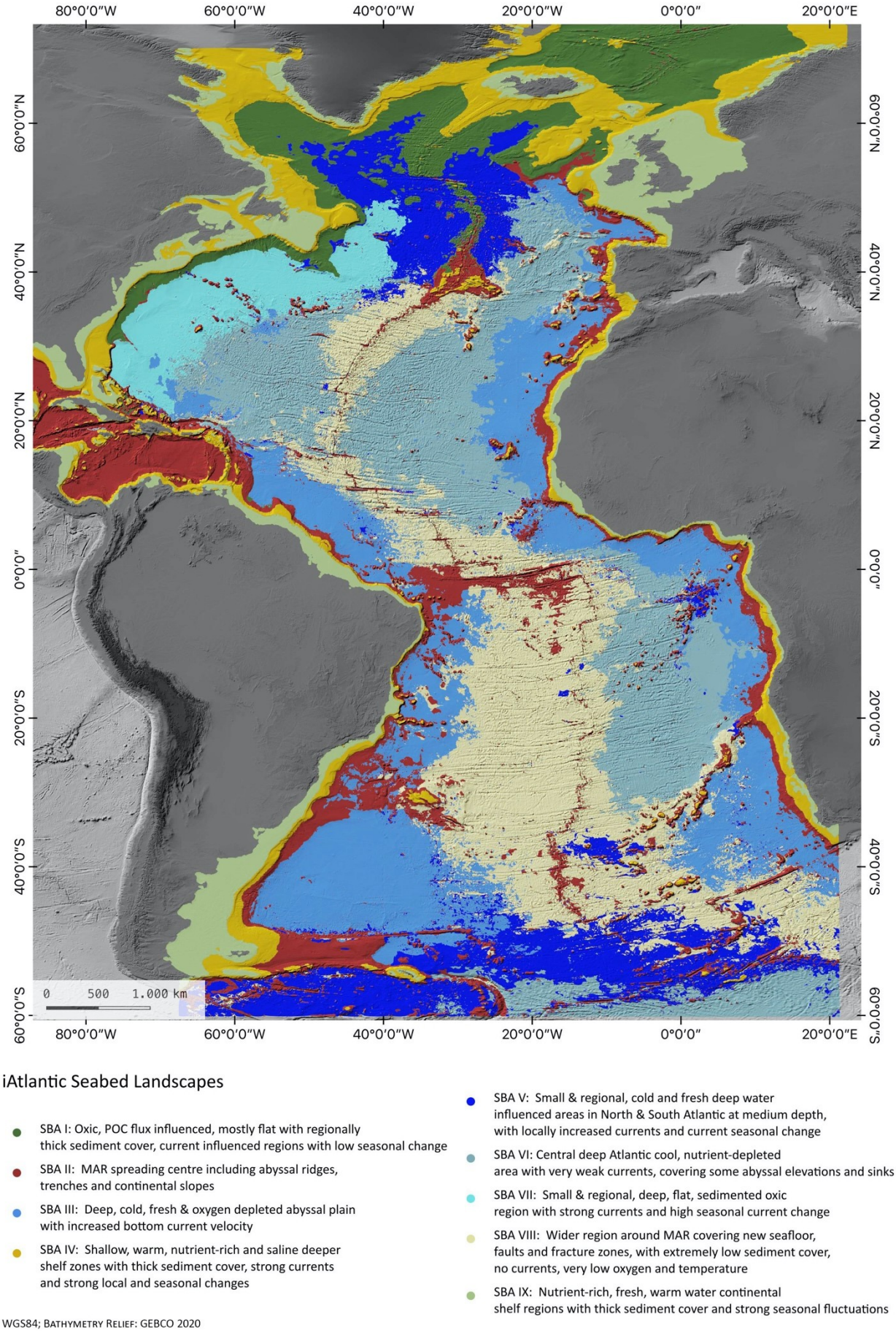

Figure 2: Atlantic Seabed Area Map

Table 1: Class description summary ordered by area covered (from the smallest to the largest).

SBA	Area [km²]	Description
7	3,472,998	SBA VII: Small and regional, deep, flat, sedimented oxic region with strong currents and high seasonal current change
1	3,998,145	SBA I: Oxic, POC flux influenced, mostly flat with regionally thick sediment cover sedimented, current influenced regions with low seasonal change
9	5,945,256	SBA IX: Oxic, POC flux influenced, mostly flat with regionally thick sediment cover sedimented, current influenced regions with low seasonal change
4	5,216,720	SBA IV: Shallow, warm, nutrient-rich and saline deeper shelf zones with thick sediment cover, strong currents and strong local and seasonal changes
5	6,002,183	SBA V: Small and regional, cold and fresh deep water influenced areas in North and South Atlantic at medium depth, with locally increased currents and current seasonal change
2	11,967,939	SBA II: MAR spreading centre including abyssal ridges, trenches and continental slopes
3	14,990,027	SBA III: Deep, cold, fresh and oxygen depleted abyssal plain with increased bottom current velocity
6	15,508,117	SBA VI: Central deep Atlantic cool, nutrient-depleted area with very weak currents, covering some abyssal elevations and sinks
8	16,128,258	SBA VIII: Wider region around MAR covering new seafloor, faults and fracture zones, with extremely low sediment cover, no currents, very low oxygen and temperature

3.2 Seabed Area Description & Morphologic Interpretation

The main class interpretation is based on the boxplots (*Figure 3*, *Figure 4*, *Figure 5* and *Figure 6*) and the therein plotted median and mean values. The boxplots give quantitative information, outlining the characteristics of each class and indicating which parameter describes the respective class in the first order. In the *Appendix*, a summary of the cluster statistics is listed in *Table 2* and *Table 3*.

To verify our SBAs, we compare them to supplementary data such like large current and upwelling systems (Speer and Zenk 1993; Rahmstorf, 2006), predicted seamount and hydrothermal vent locations (Yesson, 2011a, b; Beaulieu and Szafrański, 2020) and debris flow along continental slope canyons (Nisbet and Piper, 1998; Krastel, 2015).

We further compared the SBAs to the seascapes described by Harris and Whiteway (2009) (*Figure 1*), to the GOODS biogeographic provinces (UNESCO, 2009) and to the EMUs found by Sayre et al. (2019). The latter have been used by Morato et al. (2021) during the EU H2020 ATLAS project, the predecessor of iAtlantic, for a comprehensive study to assess their suitability for a species distribution model (SDM). As iAtlantic builds on ATLAS in certain parts, taking up on those studies is essential. Harris and Whiteway (2009) used a clustering approach (isoclass) on sea floor data which is most similar to ours. Hence, this comparison is discussed a little further. Sayre et al. (2019) also used a similar technique (KMeans) but applied in 3D on the water column which makes it difficult to directly compare to sea floor zones. The same applies to GOODS, which is based on an expert approach. Thus, those two classifications are only mentioned but not further discussed. In the *Appendix*, *Table 4* lists the SBAs we found against those of Harris and Whiteway (2009), Sayre et al. (2019) and GOODS to give an approximate association. Also, only major matching areas are included; those that have minor overlap are being ignored to avoid confusion. In *Table 5*, the input parameters of all aforementioned classifications are listed.

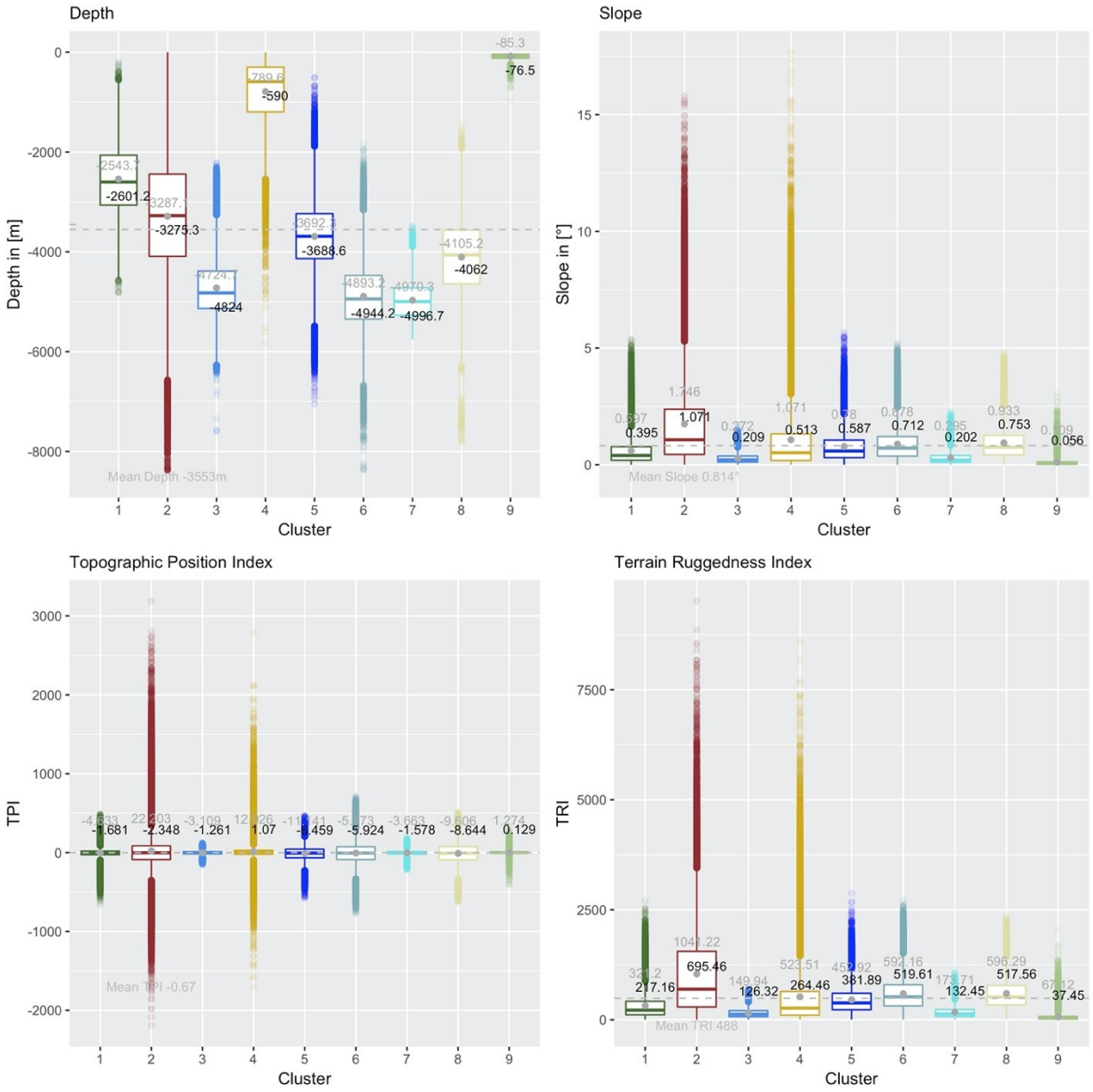

Figure 3: Boxplots outlining the SBA characteristics

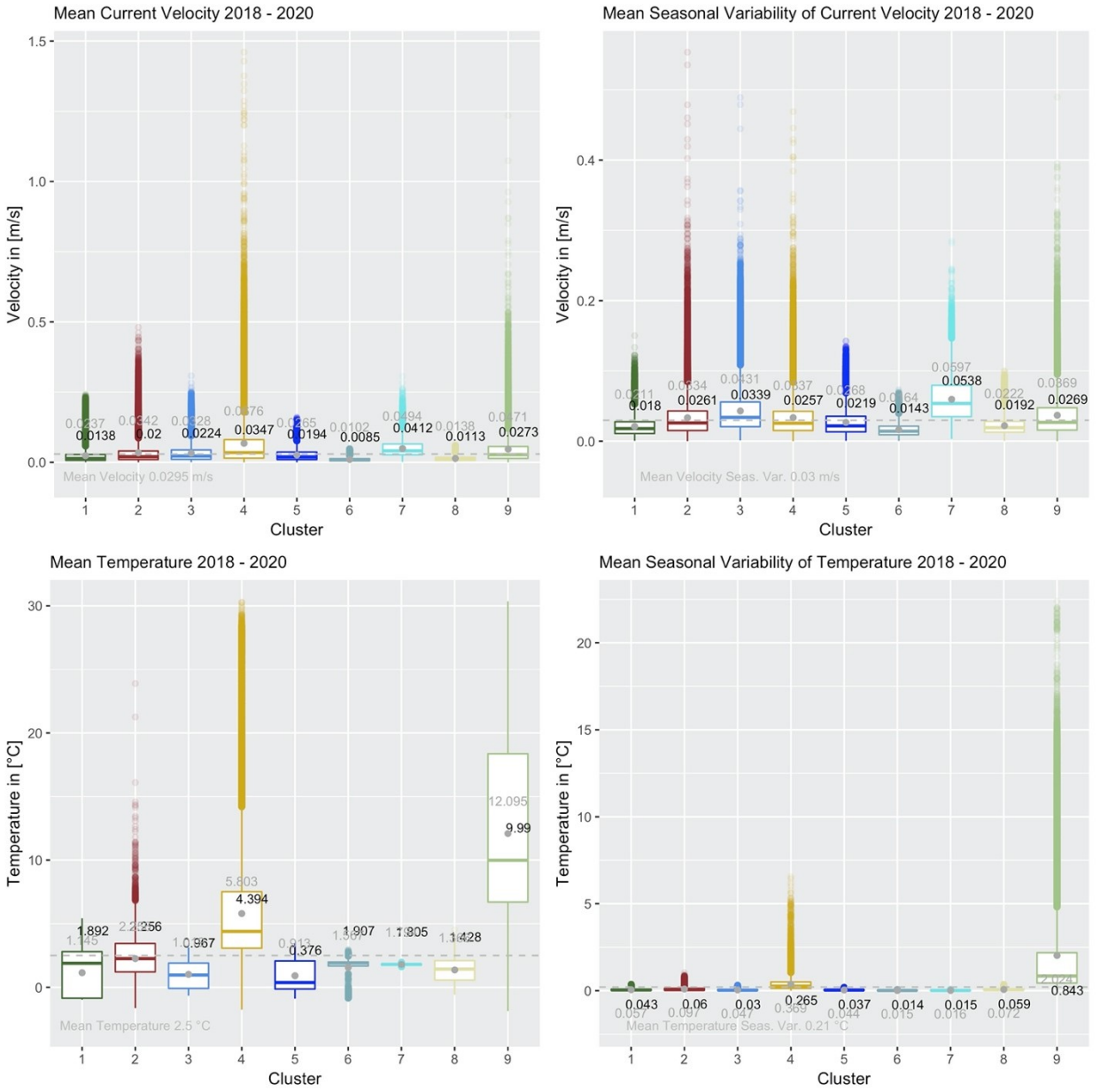

Figure 4: Boxplots outlining the SBA characteristics (cont.)

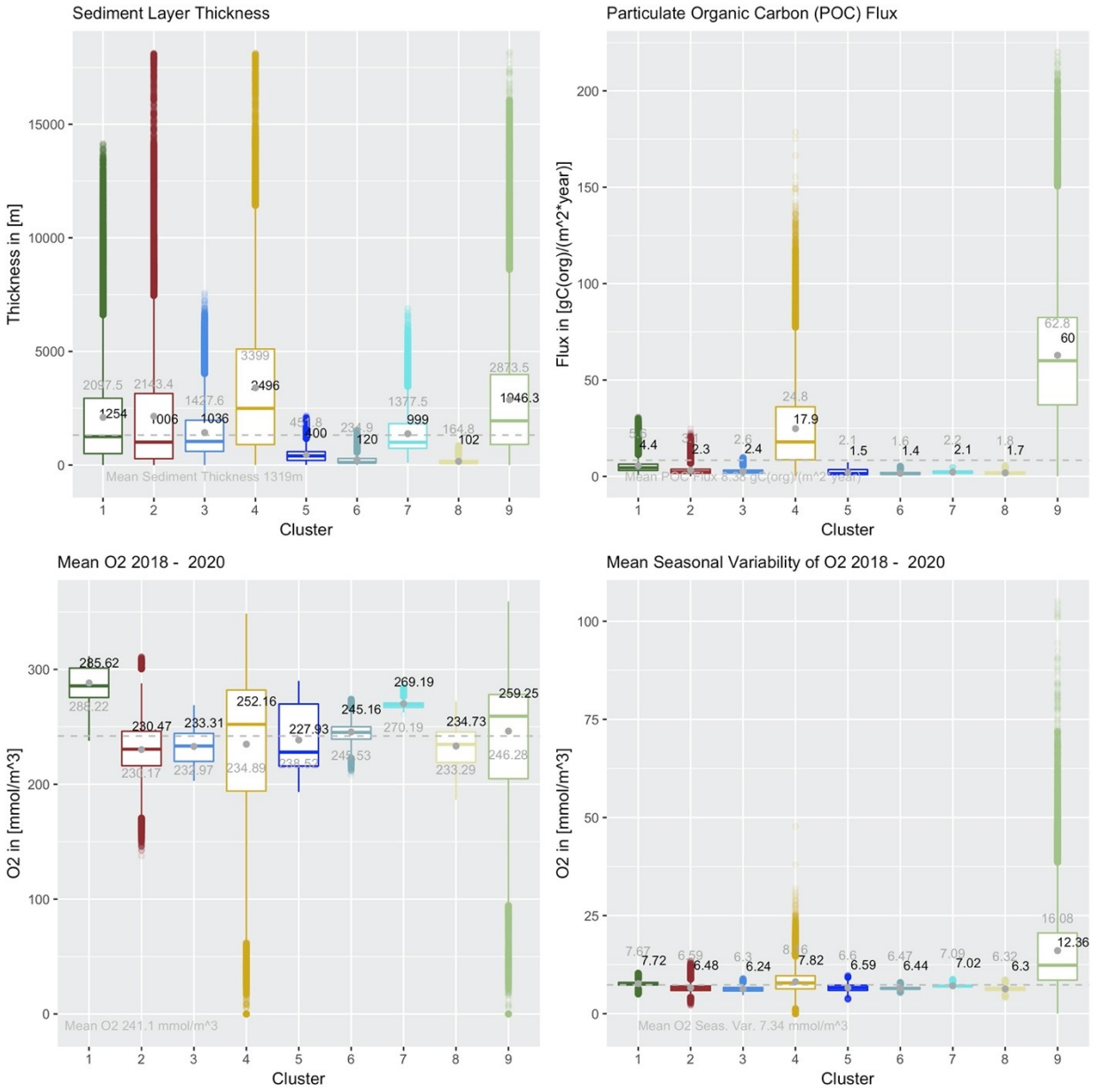

Figure 5: Boxplots outlining the SBA characteristics (cont.)

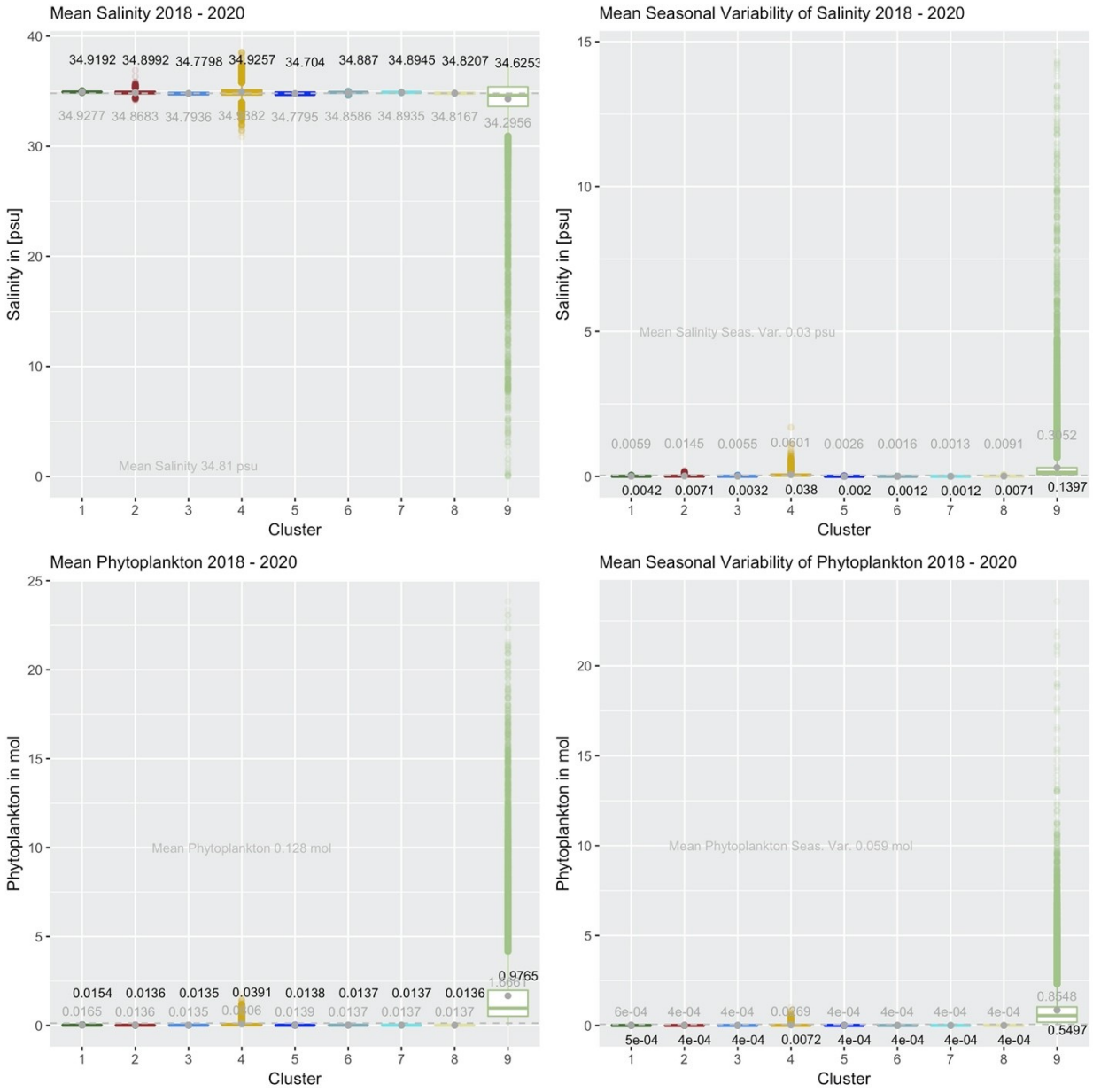

Figure 6: Boxplots outlining the SBA characteristics (cont.)

SBA I: Oxic, POC flux influenced, mostly flat with regionally thick sediment cover sedimented, current influenced regions with low seasonal change

Geography:
SBA I spreads over the continental slope at the beginning of the abyssal plain. It is **focussed mainly on the North Atlantic** with a very small patch off the coast of Guyana.

Variable brief:

- medium depth
- **low slope & TRI with high local values**
- low negative TPI
- average sediment thickness with **very high local values**
- low to average POC flux with some local higher values
- **very high oxygen** and low seasonal variability
- low velocity and seasonal variability with **very high local values**
- **chilly temperature** and low seasonal variability
- increased salinity and low to no seasonal variability

- low phytoplankton and low to no seasonal variability

Highlights & Relation to supplementary data:
SBA I is outlined by very little seasonal change while incorporating highly oxic regions. This may be explained by the influence of nearby water convection zones, such as in the Labrador and Greenland Sea, where fresh North Atlantic Deep Water (NADW) forms (Rahmstorf, 2006) (*Figure 10*). SBA I contains areas of local current systems, such as over the Greenland-Scotland-ridge complex, where currents and their seasonal changes are known to be strong (e.g. the East Greenland boundary current) (Mauritzen, 1996; Rahmstorf, 2006; Våge et al., 2011; Semper et al., 2020). Moreover, SBA I covers the area in the Labrador sea, where new water is formed (North Atlantic Deep Water, NADW), which is indicated by the cold temperature and the very high O_2 content (Rahmstorf, 2006). High local sediment thickness values may point towards debris flows through continental rise canyons (Nisbet and Piper, 1998; Krastel, 2015).

SBA II: MAR spreading centre including abyssal ridges, trenches and continental slopes

Geography:
SBA II is found in the entire Atlantic and also covers basins like the Gulf of Mexico and the Caribbean Sea. It is fairly coherent along coasts and the continental rise zone and patchier towards the Mid- Atlantic Ridge (MAR) and the abyssal plain. It corresponds in wide parts with the spreading centre of the MAR.

Variable brief:
- medium to deeper depth
- generally large slope and TRI with local very large values
- increased TPI with very high local minima & maxima
- generally average to low sediment thickness with local highly sedimented regions
- low POC flux with some local higher values
- very low oxygen and very low seasonal variability with some higher local values
- average to medium current velocity and average seasonal variability
- moderate to average temperature and low seasonal variability with regionally very warm temperatures
- average salinity with low to no seasonal variability
- low phytoplankton at low to no seasonal variability

Highlights & Relation to supplementary data:
Geomorphologically, SBA II mainly includes continental rise and abyssal areas with hardly sedimented rough terrain and steep slopes. The locally thick sediment layer point towards debris flows through continental slope canyons (Nisbet and Piper 1998; Krastel 2015). It corresponds well to the spreading centre of the MAR. SBA II also partly agrees with listed hydrothermal vent fields (Beaulieu & Szafrański 2020) and predicted seamounts (Yesson, 2011a, b) (*Figure 7*). It further includes the Gulf of Mexico and the Caribbean basin, probably due to prevailing low oxygen conditions.

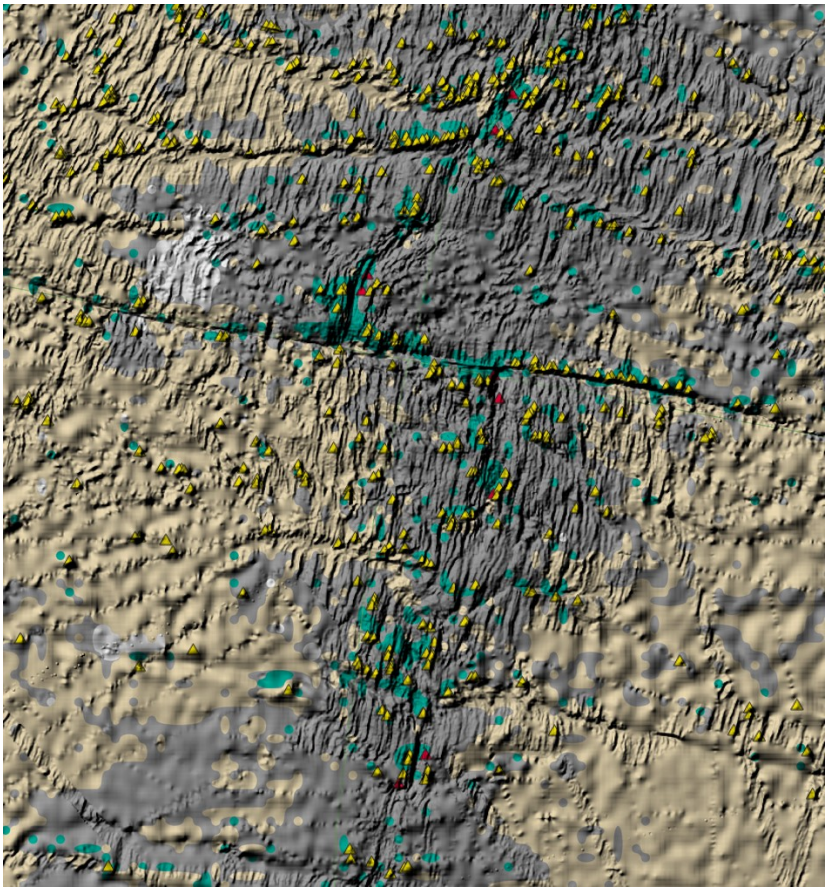

Figure 7: SBA II (in green) along with seamount (yellow, derived from Yesson, 2011a, b) and hydrothermal vent (red, derived from Beaulieu and Szafrański, 2020) locations at Kane fracture zone. Background relief: GEBCO, 2020.

SBA III: Deep, cold, fresh and oxygen depleted abyssal plain with increased bottom current velocity

Geography:
SBA III covers the deep sea abyssal plain and plateaus in the Central and South Atlantic and in the eastern North Atlantic.

Variable brief:

- very deep water
- very small slope & TRI
- slightly negative TPI
- average to low sediment thickness
- very low POC flux
- low oxygen and seasonal variability
- average to increased current velocity and seasonal variability
- very cold water with low to no seasonal variability
- low salinity with low to no seas variability
- low phytoplankton with low to no seasonal variability

Highlights & Relation to supplementary data:
SBA III covers the flat margins of the abyssal plain of the South towards the Central Atlantic. In combination with the very cold temperatures, this accounts for the influence of Antarctic Bottom Water (AABW) (Speer and Zenk 1999; Rahmstorf, 2006; Johnson, 2008) (*Figure 8*). It further includes deep sea plateaus, as e.g. around Walvis ridge, where SBA II covers the flanks but SBA III sits on the flat tops of the rises (*Figure 9*). The general low O_2 content may account for oxygen depletion of AABW on its way north. In the western

section of the North Atlantic, SBA III is superseded by the SBA VII, as this is the travel route of oxygen rich NADW (*Figure 10*).

Along with strong currents and their high seasonal change, it may also be related to eastern Atlantic upwelling regions. This process is often connected to oxygen minimum zones (OMZ) at the sea floor, induced by sinking organic matter decomposition (Diaz et al., 2013; Kaempf and Chapman, 2016).

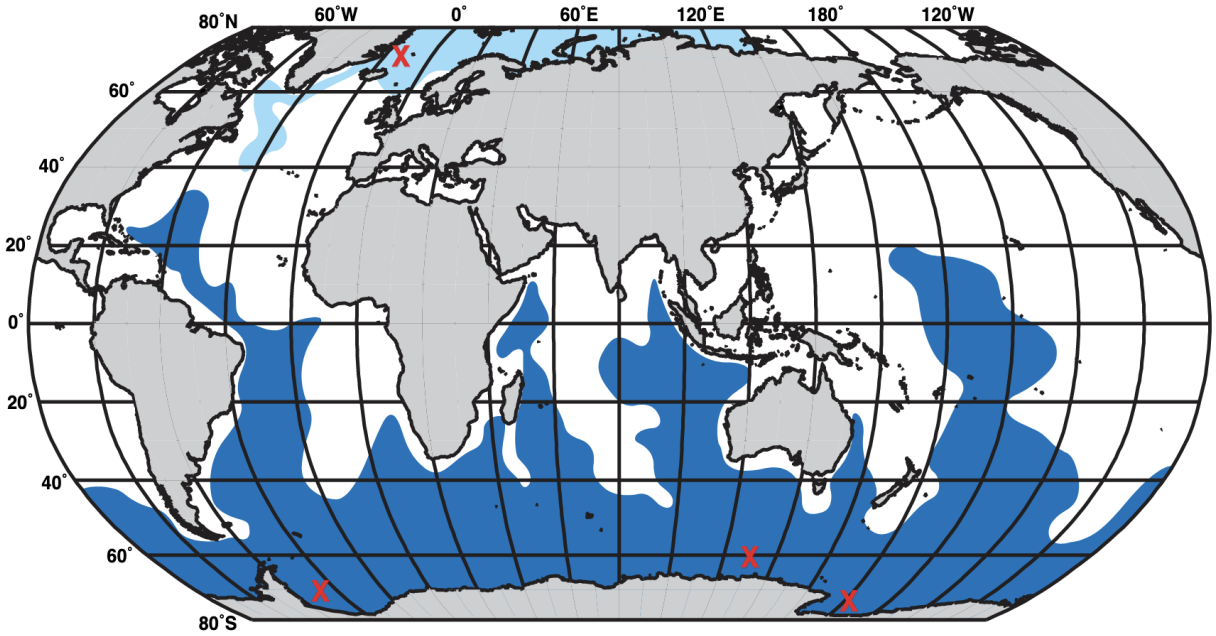

Figure 8: Global distribution of AABW. From Talley (1999) in Rahmstorf (2006).

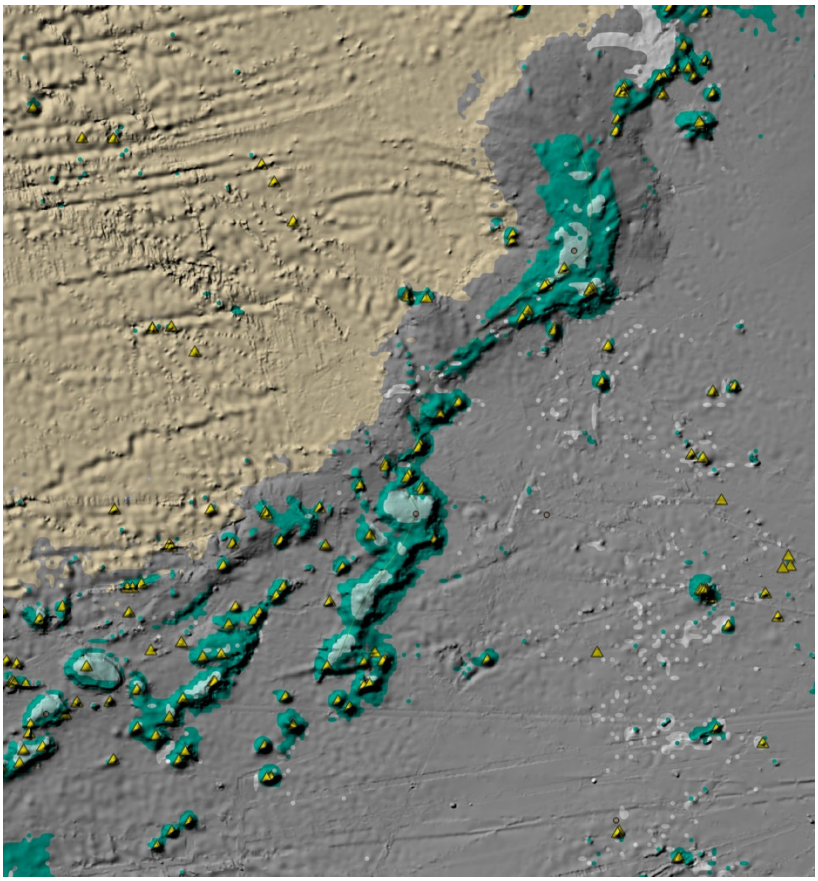

Figure 9: SBA II (in dark green) and SBA III (light green) at Walvis ridge. Seamounts are depicted as yellow triangles and derived from Yesson, 2011a, b. Background relief: GEBCO, 2020.

SBA IV: Shallow, warm, nutrient-rich and saline deeper shelf zones with thick sediment cover, strong currents and strong local and seasonal changes

Geography:
SBA IV covers continental slope and deep shelf regions of the entire Atlantic, also around rises (island arcs, ridges). Coastward, it is adjacent to SBA IX.

Variable brief:

- generally **very shallow** with some deep regions
- average slope, TRI, TPI with locally **very high values**
- very **thick sediment layer**
- very **high POC flux**
- generally average to **high oxygen** with **local oxygen minimum zones** and average seasonal variability
- average to **high current velocities and seasonal variability** with very large local values
- **warm water with very high local temperatures** at average seasonal variability
- increased salinity with regions of very high and regions with very low salinity (fresh water influence) and high seasonal variability
- increased phytoplankton and seasonal variability

Highlights & Relation to supplementary data:
SBA IV mostly spreads over shallow, warm water shelf regions with increased phytoplankton and POC flux. The high average O_2 values indicate fresh water influence by river outflows, like e.g. in the Gulf of Saint Laurent. Strong local currents and their seasonal change can be related to boundary current systems like the East Greenland current or overflow areas as the Greenland-Scotland-ridge complex (Mauritzen, 1996; Rahmstorf, 2006; Våge et al., 2011; Semper et al., 2020).

SBA V: Small and regional, cold and fresh deep water influenced areas in North & South Atlantic at medium depth, with locally increased currents and current seasonal change

Geography:
SBA V is scattered over deep Atlantic basin and rather concentrated in the North and South, less in Central Atlantic.

Variable brief:

- medium depth with some very deep and some very shallow regions
- average slope & TRI with **high local values**
- **high negative TPI** with also **high positive** and **low negative** values
- very low sediment cover
- very low POC flux
- average oxygen with a wide value distribution and low seasonal variability
- low to average current velocity with low seasonal variability
- **very cold** with low to no seasonal variability
- **low salinity** with low to no seasonal variability
- low phytoplankton with low to no seasonal variability

Highlights & Relation to supplementary data:
SBA V has two main patches, one located in the South, and one in the North Atlantic. There it covers rough terrain including some seamounts and fracture zones (Yesson, 2011a, b, IHO-IOC GEBCO 2021). The separation into North and South can be related to a possible influence of water formation which takes place in the Labrador basin (North Atlantic Deep Water, NADW) as well as in the Weddell Sea (Antarctic, AABW) (Rahmstorf, 2006) (*Figure 10*). This also matches with the cold temperatures. At first sight, the

relatively low O_2 seems contradicting. However, SBA V is not directly located in the water formation areas but adjacent to SBA I in the North. Hence, oxygen depletion has taken place already.

SBA VI: Central deep Atlantic cool, nutrient-depleted area with very weak currents, covering some abyssal elevations and sinks

Geography: SBA VI covers large patches in the Central abyssal Atlantic where terrain is a little rougher. It is adjacent to SBA III in the North and SBA VIII in the South. In the South Atlantic it only covers the eastern abyssal area of the MAR whereas up north, it spreads east and west, with the western fragment being slightly larger.

Variable brief:

- very deep with some very deep and some shallower regions
- average slope and locally increased TRI
- high negative TPI with also very high positive and very low negative values
- very low sediment cover
- very low POC flux
- average oxygen and low to no seasonal variability
- low to no current velocity and seasonal variability
- cold to average temperature with locally very cold temperatures and low to no seasonal variability
- average salinity and low seasonal variability
- low phytoplankton with low to no seasonal variability

Highlights & Relation to supplementary data:
SBA VI is mostly adjacent to SBA VIII, located in the wider section around the MAR. This and the thin sediment cover points towards newer sea floor which is underpinned by the inclusion of transform faults and fracture zones, e.g. the Fifty-Twenty or Kane Fracture zone in the Central Atlantic. The two patches of SBA VI in the central Atlantic are further located in upwelling zones as shown in ***Figure 10***.

SBA VII: Small and regional, deep, flat, sedimented oxic region with strong currents and high seasonal current change

Geography:
SBA VII is concentrated in the abyssal plain of the North America basin

Variable brief:

- very deep
- low slope & TRI
- very low negative TPI with very high positive and negative local values
- average sediment thickness with regionally thicker cover
- very low POC flux
- very high oxygen and average seasonal variability
- high current velocity and very high seasonal variability
- cool water with low to no seasonal variability
- slightly increased salinity and low seasonal variability
- low phytoplankton with low to no seasonal variability

Highlights & Relation to supplementary data:
SBA VII is quite small and regional, located in the deep abyssal plain and in the main influence zone of NADW. High O_2, cold water and seasonal change of current velocity underpin this assumption (Rahmstorf, 2006) (***Figure 10***).

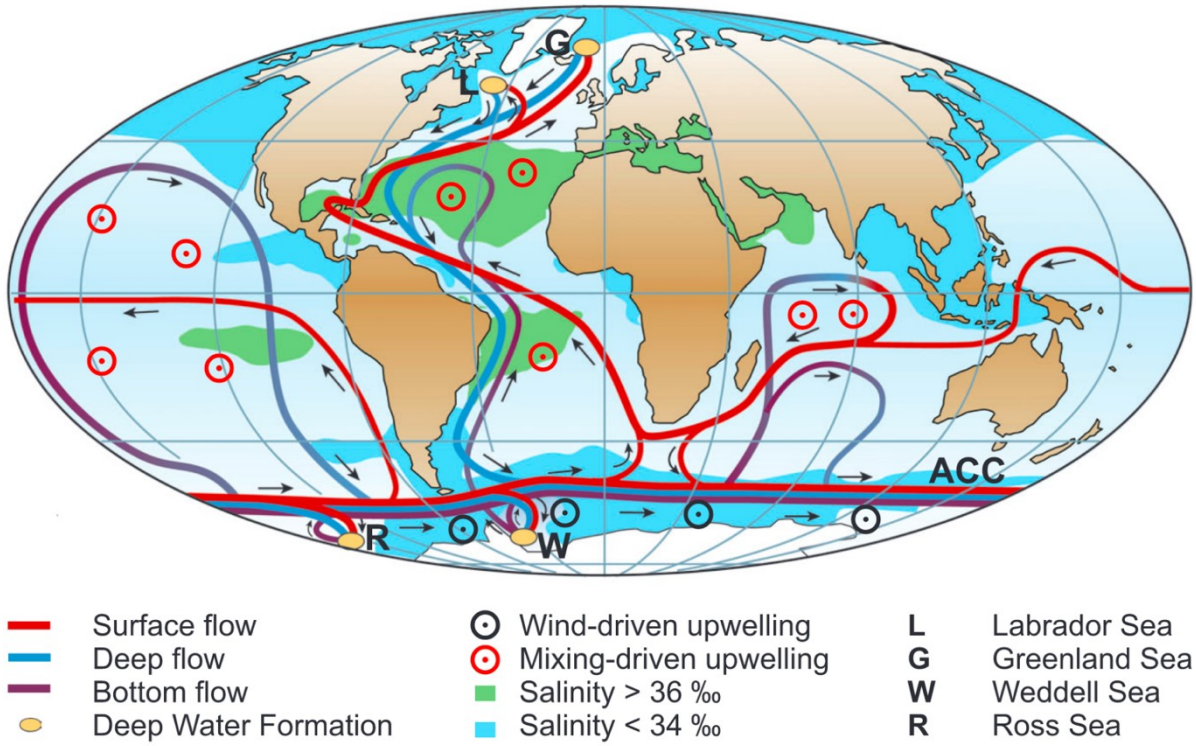

Figure 10: Global Ocean Circulation and Water Formation Areas (Rahmstorf, 2006).

SBA VIII: Wider region around MAR covering new seafloor, faults and fracture zones, with extremely low sediment cover, no currents, very low oxygen and temperature

Geography:
SBA VIII covers the region around the MAR, an area which is narrower in the North Atlantic and widening and shifting west towards the south. It is adjacent to SBA VI and SBA II.

Variable brief:

- deep water with very shallow and **very deep areas**
- average slope with **high local values**
- increased **TRI with high local values**
- negative TPI with high positive and negative values
- **very low sediment** cover
- low POC flux
- **very low oxygen** with low seasonal variability
- **very low current velocities** and seasonal variability
- **cold water** with low to no seasonal variability
- average salinity and low seasonal variability
- low phytoplankton with low to no seasonal variability

Highlights & Relation to supplementary data:
As SBA VI, SBA VIII includes areas with rough terrain in the form of transform faults and fracture zones, as it also spreads over the wider MAR region. Low sediment layer thickness accounts for newer seafloor. However, on the contrary to SBA VI, temperatures, current velocities and oxygen are lower as well as their seasonal changes. This may be explained by missing influence of deep currents like AABW or upwelling regions.

SBA IX: Nutrient-rich, fresh, warm water continental shelf regions with thick sediment cover and strong seasonal fluctuations

Geography:
Hemming shallow water continental shelf regions, SBA IX spreads along the Atlantic's adjacent coastal areas.

Variable brief:

- very **shallow water**
- very low slope and TRI
- very low positive TPI
- **thick sediment cover**
- **very high POC** flux
- average oxygen with **very low local values** and very high seasonal variability
- average current velocities and seasonal variability with very high local values
- **very warm water** and very high seasonal variability
- **very low salinity** and seasonal variability with very low local values
- very **high phytoplankton** and seasonal variability

Highlights & Relation to supplementary data:
SBA IX covers the part of the sea floor which is in the photic zone, emphasised by the very high POC flux and phytoplankton values. Strong seasonal change as well as the high current velocity seasonal change might indicate influence by wind-driven currents and coastal upwelling (Kaempf and Chapman, 2016). This process is often connected to OMZ at the sea floor, induced by sinking organic matter decomposition (Diaz et al., 2013; Kaempf and Chapman, 2016). Hence, the locally extremely low oxygen values may be related to this phenomenon. In the area around the Gulf of Mexico and Cheasapeake Bay, the low oxygen concentration could also be related to eutrophication-induced coastal hypoxia (Levin et al., 2009). High local salinity values as well as generally high seasonal changes can be related to fresh water influence by river outflows. On the Argentine shelf, the Malvinas western boundary current induces seasonal variability and fluctuations in temperature, salinity, oxygen, and currents. The latter may also be related to high amplitude tides and upwelling (Matano et al., 2010).

3.3 Error and Limitation Analysis

Despite the fact that multivariate classifications are more objective than hierarchical methods, unsupervised analyses can still bear error sources that are not visible at first sight but must be considered when using them.

Although a density estimation and model-based clustering approach seems suitable for this kind of high dimensional and complex data, it is the input data quality that needs to be looked at. The most prominent quality reducing factors are differences in scale, especially when dealing with multiple data sources. This holds true for vertical as well as for horizontal resolution. At depths > -1,000 m, CMEMS model data products have a very low vertical resolution of approximately 450 m (Lellouche et al., 2019). Hence, they only give a very rough approximation about the conditions prevailing in those depths or at the sea floor. Nevertheless, they are still are amongst the best of their type. Local small-scale (vertical) variation (e.g., in temperature, caused by hydrothermal vent fields) will hardly be caught. Given that ground truth sea floor data are scarce in the deep sea, we considered the last depth level as defined by CMEMS to be sea floor. This induces a huge vertical uncertainty, which cannot be resolved with the present data and models, but must be noted. Bathymetry, on the other hand, is a sea floor layer by nature. Hence, we are essentially setting different depth zones as equal: those directly at the sea floor (e.g., bathymetry), and the others in a vertical range between sea floor level and 450 m above it (CMEMS model data).

Horizontal resolution is another constraint and is mainly attributed to limited data availability. For this analysis, we scaled everything to the CMEMS physical data product resolution of 1/12° (around 8 km at the equator (Lellouche et al., 2019)), which required downscaling the CMEMS biological product and upscaling the bathymetry data. Downscaling data of originally lower resolution induces inaccuracies that are difficult to assess. Another option would have been to upscale all data to the lowest resolution, which in this case was ¼° (of the CMEMS biological product). However, we opted against this option, as the information loss would have been intolerably high considering the fact that oxygen and phytoplankton are the only data of this low resolution. Notably, even 1/12°, or 8 km, is a very coarse scale and does not resolve many small fluctuations and features that might be of importance (e.g., hydrothermal vent fields or small submarine volcanoes). An approach to obviate this deficiency could be to use a nested classification, running multiple cluster algorithms on the existing classes as performed in Hogg et al. (2016). This would refine the original clusters and split them into smaller parts, but would, of course, not change the initial data resolution. Both downscaling from low to high resolution as well as the reverse can be critical; this happens because high-resolution data naturally inherit more value variance that is passed on when resampled to coarser resolution, thus affecting the latter during the analysis. To partially accommodate this, we scaled the data and chose model-based clustering, as it is robust towards different variances (e.g., Scrucca et al., 2016).

Higher resolution ocean models (e.g. VIKING20x (Getzlaff and Schulzki, 2009) or INALT (Schwartzkopf et al., 2019)) on a basin wide or even global scale would significantly improve those kinds of seabed clustering. To date, those models are only locally (e.g. North Atlantic) available and usually have a very fine resolution at the sea surface which also becomes coarse towards the sea floor. However, research and computation power are advancing and so are the models. For example, iAtlantic's WP1 uses VIKING20x and INALT to better understand the global ocean circulation, and aims at refining them by placing new sensors to existing moorings (the measurements of these sensors essentially feed those models).

4. Discussion & Outlook

4.1 General Observations

Generally, the SBAs we found have individual identifying characteristics and are well distinguishable from each other as shown in most of the value distributions of the boxplots. We found seven SBA located in the abyss and deep sea (SBAs I, II, III, V, VI, VII and VIII) and two that define coastal and (deeper) shelf areas (SBAs IV and IX). Many of the identified areas seem strongly impacted by deep water currents such as the NADW and the AABW. We also observed a separation into a Northern and a Southern hemisphere, which could also be related to bottom currents and water formation areas. This is underpinned by the expert knowledge based GOODS classification whose authors also found a strong separation into North and South Atlantic (*Table 4*, UNESCO, 2009; Morato et al., 2021). SBA II sort of sticks out being mainly formed by the topographic variables depth, slope, TRI and TPI, following the MAR as well as steep continental slopes, including seamount, ridge and trench areas (e.g. Walvis Ridge). All other SBAs do not seem to be too much related to topography, which is in contrast to Harris and Whiteway (2009), whose seascapes seem to be mostly defined by geomorphologic variables (i.e. slope) as they did not take into account currents for example.

Some of the SBAs seem harder to distinguish regarding the parameters in the boxplots and their geographic coverage. For example, SBA VI and SBA VIII have quite similar boxplots for the hydrographic parameters and also slope, TPI and TRI are somewhat corresponding. Both are mixed SBAs in a sense that they are defined by both morphologic and hydrographic parameters. Both cover the centre part of the Atlantic from south to north, with SBA VIII covering a slightly narrower region around the MAR, especially in the North Atlantic. The two major differences are depth and oxygen, whereby SBA VI covers deeper areas containing more O_2 due to the influence of NABW. The influence of deep currents is noticed in many of the identified SBAs and along with topography, those seem to be the two key factors thriving the deep

sea environment. To find out whether those are the only major influencing parameters, a more detailed assessment is necessary on those mixed SBAs to make finer separations. This could be a nested, hierarchical approach which separates morphological, chemical, hydrographical and biologic components of those SBAs and classifies them again according to those components in a second step. Consulting higher resolution data would be beneficial to evaluate whether small scale variations, i.e. from hydrothermal vent fields, would change the local chemical composition and the ambient water temperature. Local hydrodynamic and morphologic conditions are also extremely important drivers for food flux and organic matter transport to the seabed. These processes however typically operate at the scale of an offshore bank or seamount and are hence not captured within this study.

We acknowledge that in reality, inter-class or inter-seascape boundaries are not solid as implied on the map, since the ocean is a dynamic and ever-changing system. Behind the scenes, the model-based clustering approach we took is based on probabilities, in a way that each sample point of the data set is associated with a certain probability of belonging to one model ('soft' boundaries) rather being fully assigned to one cluster as it is the case with K-Means for example. However, for an easier interpretation and further implementation, we draw hard cluster boundaries on the map.

It is difficult to answer whether the classified environmental entities contain distinct species assemblages: in addition to physical variables, life-history traits and biological interactions will influence biogeographic patterns. Even if the physical environment is similar, species and assemblages may differ. This issue is widely discussed in Morato et al. (2021), who compared broad-scaled existing classifications to results of species distribution models to find that neither of the classifications matches their SDM boundaries. However, it can be expected that in higher resolution models, areas with similar environmental characteristics may host ecosystems with similar structures and functions. While individual species may not be the same, species with similar traits and functional behaviour may populate areas with similar physical environments (e.g., burrowing fauna in heavily sedimented areas or filter-feeders in complex, rocky environments) (e.g. McGill et al., 2006; Zeng, 2020). From a biodiversity management perspective, such spatially explicit delineation of potential ecosystem functions (and therefore services) will still be of high value.

Morato et al. (2021) have made steps towards integrating such biogeographic province classification maps into environmental niche modelling (e.g. species distribution models (SDM) or habitat suitability models (HSM)). In their complex work, they compared the two seafloor bioregion models EMU and GOODS to an SDM. Although their results show only very little to hardly any agreement of the SDM's with the bioregions' boundaries, they still outline a valuable approach and a possibility of implementing those kinds of classification into species prediction related work. To effectively predict and relate species to environmental conditions, classifications and data at a much finer scale must be available (Lim et al., 2021). But the combination of high-resolution classifications and SDMs or HSMs is a very promising task, capable to essentially support marine area-based management and spatial planning work (Lim et al., 2021; Morato et al. 2021).

4.2 Comments on the seascapes by Harris and Whiteway (2009), GOODS (UNESCO, 2009) and EMU (Sayre et al., 2019)

When comparing the SBAs we identified to preceding studies, some of our SBAs (III, V, VII) can be 'translated' into one single seascape (10), others (e.g. SBA VIII) correspond to more than one seascape (5, 7 and 9). This might be due to the fact that we used additional non-morphologic parameters like current speed, POC flux, etc., higher resolution data (1/12° for SBAs, 1/10° for seascapes) and more recent data. We have not included primary production into the classification, as it is a variable mostly determining the ocean surface and the upper water column until a depth of around -350 m (CMEMS, 2021). Harris and Whiteway (2009) did not take any seasonal variability into account, a measure which, on the other hand, we considered crucial for currents, salinity, temperature and oxygen concentration. They further excluded salinity, arguing that salinity variation at sea floor depths is very low. This may be correct in the deeper

parts of the Atlantic, but our results show that salinity values and seasonal variability do play a role in the shallower SBA IX region, to be precise, which corresponds to the excluded area. In addition to depth and slope, we also included TPI and TRI. Furthermore, the authors defined seascapes on a global scale and, depending on the principal parameters that define the respective seascape, those may vary across the global ocean compared to the Atlantic basin. They also excluded areas shallower than -200 m. Another major difference is that we applied a different clustering technique, one which allows for cluster shapes other than only spherical. To assess this issue in detail, a comparison of the two methods, GMM and KMeans, on the same data set would be necessary. However, we do not have a lot of ground truthing for this kind of comprehensive and multivariate area composition of the deep sea. Hence, identifying the best technique is a complex task.

With regards to the comparison against the other two classifications GOODS (UNESCO, 2009) and EMU (Sayre et al., 2019), it is difficult to make clear statement. GOODS is a purely expert-based (subjective classification), and EMUs are three dimensional entities which are difficult to project onto the seafloor. Hence, a comparison has to be handled with caution. Except for the very small SBAs I and VII, all SBAs correspond to more than one biogeographic region (GOODS) or EMU, respectively (*Table 4*). As both EMUs and the GOODS areas are quite large in their extent, several of those regions are almost as large as the entire Atlantic basin, which makes a direct comparison obsolete. However, it might be extremely useful to consult more than one classification (e.g. in marine spatial planning or MPA network designation processes) to illuminate several aspects of the same area.

4.3 Methodological constraints and data limitation

Another crucial limitation which may influence the classification is the predictor variable selection itself. This issue has been widely discussed (e.g., Harris and Whiteway, 2009; Howell, 2010; Watling, 2013) and several determinants have been agreed as being good representatives of the ocean environment. In this study, we focused on morphological and hydrographical parameters, largely leaving out biologic measures, as our aim was to define submarine landscapes (e.g. Pearman et al., 2020). However, the ocean and its inhabitants form a coherent system and human impact (e.g., mining, fishing, etc.) has an influence on these ecosystems. Hence, data selection has to be probably expanded to encompass the full range of factors that affect the seafloor habitat. A more holistic approach, also with respect to marine protected area designation, would be to include a larger span of environmental data, but also information on natural resources abundances, fishing grounds, etc., such as bottom-trawling fishing activities that negatively impact the benthic environment (Eggleton et al. 2018; Ferguson et al., 2020).

5. Conclusion

This work presents a marine landscape map of the Atlantic sea floor based on an unsupervised, multivariate statistics cluster analysis. We found nine seabed areas in total, each of them being unique and differently defined by oceanographic and morphologic determinants. Unsupervised cluster analyses have the advantage of providing an objective view on the ocean environment, stepping away from human-defined hierarchical categorisations towards an unbiased understanding of sea floor ecosystem coherence.

The usefulness of this exercise can also be examined with respect to the global seascape map made by Harris and Whiteway (2009). Our approach brings an updated, broad picture of the Atlantic sea floor basin into the discussion on sustainable management of ocean space and resources, particularly in Areas Beyond National Jurisdiction, which is a topical discourse that has been happening and still is ongoing, against the drawback of increased use of the marine environment outside Exclusive Economic Zones (e.g., deep-sea mining, and high seas fisheries). Although there is no official procedure for implementation yet (this is another crucial field to be examined), broad-scale marine landscapes like this can be a helpful tool for the

designation of marine protected areas (MPAs), for area-based management as well as for spatial marine planning (e.g. Magali et al., 2021).

Generally, depending on the clustering technique applied and the selection of input parameters, the results can be very different, highlighting the complexity and variability of the ocean realm (e.g. Pearman et al., 2020). An in-depth assessment and comparison would be needed at this point. As there is not the one 'true' arrangement of marine bio-physio-chemical-morphologic regimes, verification can only take place via ground truthing – and even this may not catch the entire complex diversity (Morato et al., 2021). Hence, depending on the purpose, a combination of several existing models may be more useful than one standalone classification.

Using more and finer-scaled data would be a major step forward and probably reveal even more unseen sides of the ocean, helping to identify biodiversity hotspots as well as vulnerable habitats. Among others, this would require full multibeam bathymetry coverage everywhere, a mission iAtlantic is also dealing with in cooperation with Seabed2030. It also demands finer scale data for the water column for variables such as temperature, salinity, oxygen, nutrients, POC flux and currents, which in turn requires high-resolution modelling (horizontally and vertically). This is already in progress, for example in the form of the VIKING20 ocean model which is being implemented within the iAtlantic WP1.

Furthermore, for iAtlantic's WP2, a basin wide approach to predict species is in progress. As a future task, it would be valuable to assess whether distribution patterns can be related to the marine landscapes we found in this study. Unfortunately, this would exceed the scope of this study and to date, the species prediction is not yet completed. iAtlantic WP6 is making efforts to address decision and policy makers in terms of ocean conservation and protection plans, where such results or combinations of results can be a supporting and informative contribution. The online platform GeoNode (http://www.geonode.iatlantic.eu/) (iAtlantic WP5), where the dataset of this study will also be published, therefore acts as a tool for sharing and distributing knowledge.

References

Altmann, A., Toloşi, L., Sander, O., Lengauer, T. (2010): Permutation importance: a corrected feature importance measure. Bioinformatics, 26, 1340–1347, https://doi.org/10.1093/bioinformatics/btq134.

Aumont, O., Ethé, C., Tagliabue, A., Bopp, L., Gehlen, M. (2015): PISCES-v2: an ocean biogeochemical model for carbon and ecosystem studies. Geoscientific Model Development, 8, 2465–2513, https://doi.org/10.5194/gmd-8-2465-2015.

Beaulieu, S.E. and Szafrański, K.M. (2020): InterRidge Global Database of Active Submarine Hydrothermal Vent Fields Version 3.4. PANGAEA, https://doi.org/10.1594/PANGAEA.917894.

Becker, J.J., Sandwell, D.T., Smith, W.H.F., Braud, J., Binder, B., Depner, J., Fabre, D., Factor, J., Ingalls, S., Kim, S.H., Ladner, R., Marks, K., Nelson, S., Pharaoh, A., Trimmer, R., von Rosenberg, J., Wallace, G., Weatherall, P. (2009): Global bathymetry and elevation data at 30 arc-seconds resolution: SRTM30 PLUS. Marine Geodesy, 32, 355-371, https://doi.org/10.1080/01490410903297766.

Brewer, C. and Harrower, M. (2021): ColourBrewer, the Pennsylvania State University. URL: https://colorbrewer2.org/#, Accessed in August 2021.

British Oceanographic Data Centre (2020): Gebco Gridded Global Bathymetry Data. URL: https://www.gebco.net/data_and_products/gridded_bathymetry_data/gebco_2020/, Accessed in August 2021.

Chune, S.L., Nouel, L., Fernandez, E., Derval, C., Tressol, M., Dussurget, R. (2020): Product User Manual for Global Biogeochemical Analysis and Forecast product GLOBAL_ANALYSIS_FORECAST_PHY_001_024. EC Copernicus Marine Environment Monitoring Service 1.6, pp. 34, Public Ref.: CMEMS-GLO-PUM-001-024.

Clark, M.R., Watling, L., Rowden, A.A., Guinotte, J.M., Smith, C.R. (2011): A global seamount classification to aid the scientific design of marine protected area networks. Ocean and Coastal Management, 54, 19-36, https://doi.org/10.1016/j.ocecoaman.2010.10.006.

Combes, M., Vaz, S., Grehan, A., Morato, T., Arnaud-Haond, S., Dominguez-Carrió, C., Fox, A., González-Irusta, J.M., Johnson, D., Callery, O., Davies, A., Fauconnet, L., Kenchington, E., Orejas, C., Roberts, J.M., Taranto, G., Menot, L. (2021): Systematic Conservation Planning at an Ocean Basin Scale: Identifying a Viable Network of Deep-Sea Protected Areas in the North Atlantic and the Mediterranean. Frontiers in Marine Science, 8, 611358, https://doi.org/10.3389/fmars.2021.611358.

Davies, C.E., Moss, D., Hill, M.O. (2004): EUNIS Habitat Classification Revised 2004. Paris: European Topic Centre on Nature Protection and Biodiversity, 127–143, http://eunis.eea.europa.eu/upload/EUNIS_2004_report.pdf.

Diaz, R.J., Eriksson-Hägg, H., Rosenberg, R. (2013): Chapter 4 – Hypoxia. Eds.: Noone, K.J., Sumaila, U.R., Diaz, R.J., In: Managing Ocean Environments in a Changing Climate, Elsevier, pp. 67-96, https://doi.org/10.1016/B978-0-12-407668-6.00004-5.

Eggleton, J.D., Depestele, J., Kenny, A.J., Bolam, S.G., Garcia, C. (2018): How benthic habitats and bottom trawling affect trait composition in the diet of seven demersal and benthivorous fish species in the North Sea. Journal of Sea Research, 142, 132-146, https://doi.org/10.1016/j.seares.2018.09.013.

EU Copernicus Marine Service: Operational Mercator Biochemical Global Ocean Analysis and Forecast System, GLOBAL_ANALYSIS_FORECAST_BIO_001_028. URL:

https://resources.marine.copernicus.eu/?option=com_csw&view=details&product_id=GLOBAL_ANALYSIS_FORECAST_BIO_001_028, Accessed in February 2021.

EU Copernicus Marine Service: Operational Mercator Global Ocean analysis and forecast system, GLOBAL_ANALYSIS_FORECAST_PHYS_001_024. URL: https://marine.copernicus.eu/node/173, Accessed in February 2021.

Ferguson, A.J.P., Oakes, J., Eyre, B.D. (2020): Bottom trawling reduces benthic denitrification and has the potential to influence the global nitrogen cycle. Limnology and Oceanography, 5, 237-245, https://doi.org/10.1002/lol2.10150.

GDAL/OGR contributors (2021): GDAL/OGR Geospatial Data Abstraction software Library. Open Source Geospatial Foundation. URL: https://gdal.org, Accessed in August 2021.

Getzlaff, K. and Schulzki T. (2018): VIKING20X_SST_5day_2000_2009. GEOMAR Helmholtz Centre for Ocean Research Kiel, https://core.ac.uk/display/163103839.

Gille, S.T., Metzger, E.J., Tokmakian, R. (2004): Seafloor topography and ocean circulation. Oceanography, 17, 47–54, https://doi.org/10.5670/oceanog.2004.66.

Harris, P.T. and Whiteway, T. (2009): High seas marine protected areas: Benthic environmental conservation priorities from a GIS analysis of global ocean biophysical data. Ocean and Coastal Management, 52, 22-38, https://doi.org/10.1016/j.ocecoaman.2008.09.009.

Harris, P.T., MacMillan-Lawler, M., Rupp, J., Baker, E.K. (2014): Geomorphology of the oceans. Marine Geology, 352, 4-24, https://doi.org/10.1016/j.margeo.2014.01.011.

Hogg, O. T., Huvenne, V.A.I., Griffiths, H.J., Dorschel, B., Linse, K. (2016): Landscape mapping at sub-Antarctic South Georgia provides a protocol for underpinning large-scale marine protected areas. Science Reports, 6, 33163, https://www.nature.com/articles/srep33163.

Howell, K.L. (2010): A benthic classification system to aid in the implementation of marine protected area networks in the deep/high seas of the NE Atlantic. Biological Conservation, 143, 1041–1056, https://doi.org/10.1016/j.biocon.2010.02.001.

IHO-IOC GEBCO Gazetteer of Undersea Feature Names. URL: https://www.ngdc.noaa.gov/gazetteer/, Accessed in August 2021.

Ismail, K., Huvenne, V., Masson, D. (2015): Objective automated classification technique for marine landscape mapping in submarine canyons. Marine Geology 363, 17–32, https://doi.org/10.1016/j.margeo.2015.01.006.

IUCN (2018): Area Based Management Tools, Including Marine Protected Areas in Areas Beyond National Jurisdiction. 9 – 11 October, IUCN Headquarters, Gland, Switzerland.

Johnson, G.C. (2008): Quantifying Antarctic Bottom Water and North Atlantic Deep Water volumes. In: Journal of Geophysical Research – An AGU Journal V113 C5, https://doi.org/10.1029/2007JC004477

Kaempf, J. and Chapman, P. (2016): The Functioning of Coastal Upwelling Systems. Upwelling Systems of the World, 31-65, https://doi.org/10.1007/978-3-319-42524-5_2.

Kavanaugh, M.T., Oliver, M.J., Chavez, F.P., Letelier, R.M., Muller-Karger, F.E., Doney, S.C. (2016): Seascapes as a new vernacular for pelagic ocean monitoring, management and conservation. ICES Journal of Marine Science, 73, 1839–1850, https://doi.org/10.1093/icesjms/fsw086.

Kharbush, J.J., Close, H.G., Van Mooy, B.A.S., Arnosti, C., Smittenberg, R.H., Le Moigne, F.A.C., Mollenhauer, G., Scholz-Böttcher, B., Obreht, I., Koch, B.P., Becker, K.W., Iversen, M.H., Mohr, W. (2020): Particulate Organic Carbon Deconstructed: Molecular and Chemical Composition of Particulate Organic Carbon in the Ocean. Frontiers in Marine Science, 7, 518, https://doi.org/10.3389/fmars.2020.00518.

Krastel, S. (2015): Interaction of large landslides and canyons off NW Africa. Submarine Canyon Dynamics, CIESM Workshop Monographs N° 47, 15-18 April, Sorrento, Italy.

Lellouche, J.M., Greiner, E., Le Galloudec, O., Garric, G., Regnier, C., Drevillon, M., Benkiran, M., Testut, C.E., Bourdalle-Badie, R., Gasparin, F., Hernandez, O., Levier, B., Drillet, Y., Remy, E., Le Traon, P.Y. (2018): Recent updates to the Copernicus Marine Service global ocean monitoring and forecasting real-time 1/12° high-resolution system. Ocean Science, 14, 1093–1126, https://doi.org/10.5194/os-14-1093-2018.

Lellouche, J.M., Le Galloudec, O., Regnier, C., Levier, B., Greiner, E., Drevillion, M. (2019): Quality Information Document for Global Sea Physical Analysis and Forecasting Product GLOBAL_ANALYSIS_FORECAST_PHY_001_024. Public Ref.: CMEMS-GLO-QUID-001-024.

Levin, L.A., Ekau, W., Gooday, A.J., Jorissen, F., Middelburg, J.J., Naqvi, S.W.A., Neira, C., Rabalais, N.N., Zhang, J. (2009): Effects of natural and human-induced hypoxia on coastal benthos. Biogeosciences, 6, 2063–2098, https://doi.org/10.5194/bg-6-2063-2009.

Lim, A., Wheeler, A.J., Conti, L. (2021): Cold-Water Coral Habitat Mapping: Trends and Developments in Acquisition and Processing Methods. Geosciences, 11, 9, https://dx.doi.org/10.3390/geosciences11010009.

Lutz, M. J., K. Caldeira, R. B. Dunbar, M. J. Behrenfeld (2007): Seasonal rhythms of net primary production and particulate organic carbon flux to depth describe the efficiency of biological pump in the global ocean, *J. Geophys. Res.*, 112, C10011, doi:10.1029/2006JC003706.

Magali, C., Vaz, S., Grehan, A., Morato, T., Arnaud-Haond, S., Dominguez-Carrió, C., Fox, A., González-Irusta, J.M., Johnson, D., Callery, O., Davies, A., Fauconnet, L., Kenchington, E., Orejas, C., Roberts, J.M., Taranto, G., Menot, L. (2021): Systematic Conservation Planning at an Ocean Basin Scale: Identifying a Viable Network of Deep-Sea Protected Areas in the North Atlantic and the Mediterranean. Frontiers in Marine Science, 8, 800, https://doi.org/10.3389/fmars.2021.611358.

Matano, R., Palma, E., Piola, A. (2010): The influence of the Brazil and Malvinas Currents on the southwestern Atlantic shelf circulation. Ocean Science Discussions, 6, 983–995, https://doi.org/10.5194/os-6-983-2010.

Mauritzen, C. (1996): Production of dense overflow waters feeding the North Atlantic across the Greenland-Scotland Ridge. Part 1: Evidence for a revised circulation scheme. Deep Sea Research Part I: Oceanographic Research Papers, 43, 769-806, https://doi.org/10.1016/0967-0637(96)00037-4.

McGill, B.J., Enquist, B.J., Weiher, E., Westoby, M. (2006): Rebuilding community ecology from functional traits. Trends in Ecology and Evolution, 21, 178-185. https://doi.org/10.1016/j.tree.2006.02.002

McQuaid, K.A., Attrill, M.J., Clark, M.R., Cobley, A., Glover, A.G., Smith, C.R., Howell, K.L. (2020): Using Habitat Classification to Assess Representativity of a Protected Area Network in a Large, Data-Poor Area Targeted for Deep-Sea Mining. Frontiers in Marine Science 7, 1066, https://www.frontiersin.org/article/10.3389/fmars.2020.558860.

Morato, T., González-Irusta, J.M., Dominguez-Carrió, C., Wei, C.L., Davies, A., Sweetman, A.K., Taranto, G.H., Beazley, L., García-Alegre, A., Grehan, A., Laffargue, P., Murillo, F.J., Sacau, M., Vaz, S., Kenchington,

E., Arnaud-Haond, S., Callery, O., Chimienti, G., Cordes, E., Egilsdottir, H., Freiwald, A., Gasbarro, R., Gianni, M., Gilkinson, K., Wareham Hayes, V.E., Hebbeln, D., Hedges, K., Henry, L.A., Kazanidis, G., Koen-Alonso, M., Lirette, C., Mastrototaro, F., Menot, L., Molodtsova, T., Durán Muñoz, P., Murton, B., Orejas, C., Pennino, M.G., Puerta, P., Ragnarsson, S.A., Ramiro-Sánchez, B., Rice, J., Rivera, J., Roberts, J.M., Rodrigues, L., Ross, S.W., Rueda, J.L., Snelgrove, P., Stirling, D., Treble, M., Urra, J., Vad, J., Watling, L., Walkusz, W., Wang, Z., Wienberg, C., Woillez, M., Levin, L.A., Neat, F., Das, D., Fauconnet, L., Viegas, C., Afonso, P., Menezes, G., Pinho, M.R., Silva, H., Rosa, A., Catarino, D., Giacomello, E., Guijarro, J., Cleland , J., Yeo, I., Xavier, J.R., Sampaio, I., Spearman, J., Victorero, L., Messing, C.G., Bilan, M., Blasco-Ferre, J., Bourillet, J. F., de Chambure, L., Davies, J.S., Frank, N., Guillaumont, B., Georgoulas, K., Berx, B., Olu, K., Ramos, M., Ramalho, L., Renones, O., Caballero, J.A., Tempera, F., Tourolle, J., Utrilla, O., van den Beld, I., Yashayaev, I., Serrano, A., Grasshoff, M., Rochette, S., Pham, C.K., Carreiro-Silva, M. (2021): EU H2020 ATLAS Deliverable 3.3: Biodiversity, biogeography and GOODS classification system under current climate conditions and future IPCC scenarios. Zenodo, https://doi.org/10.5281/zenodo.4658502.

Nisbet, E., and Piper, D. (1998): Giant submarine landslides. Nature, 392, 329–330, https://doi.org/10.1038/32765.

Paul, J. (2019): Product User Manual for Global Biogeochemical Analysis and Forecast Product GLOBAL_ANALYSIS_FORECAST_BIO_001_028. Public Ref.: CMEMS-GLO-PUM-001-028.

Pearman, T.R.R., Robert, K., Callaway, A., Hall, R., Lo Iacono, C., Huvenne, V.A.I. (2020): Improving the predictive capability of benthic species distribution models by incorporating oceanographic data – Towards holistic ecological modelling of a submarine canyon. Progress in Oceanography, 184, 102338, https://doi.org/10.1016/j.pocean.2020.102338.

Press, W.H., Teukolsky, S.A., Vetterling, W.T., Flannery, B.P. (2007): Section 16.1. Gaussian Mixture Models and k-Means Clustering. In: Numerical Recipes: The Art of Scientific Computing. Cambridge University Press, Cambridge, United Kingdom.

QGIS Development Team (2020): QGIS Geographic Information System. Open Source Geospatial Foundation Project, URL: http://qgis.osgeo.org, Accessed in August 2021.

R Core Team (2018): R: A language and environment for statistical computing. R Foundation for Statistical Computing, Vienna, Austria.

Rahmstorf, S. (2006): Thermohaline Ocean Circulation. Eds.: Elias, S.A., In: Encyclopedia of Quaternary Sciences, Elsevier, Amsterdam, Netherlands.

Riley, S., Degloria, S., Elliot, S.D. (1999): A Terrain Ruggedness Index that Quantifies Topographic Heterogeneity. International Journal of Science, 5, 23-27, https://www.researchgate.net/publication/259011943_A_Terrain_Ruggedness_Index_that_Quantifies_Topographic_Heterogeneity.

Roff, J.C., Taylor, M.E., Laughren, J. (2003): Geophysical approaches to the classification, delineation and monitoring of marine habitats and their communities. Aquatic Conservation: Marine and Freshwater Ecosystems, 13, 77-90. https://doi.org/10.1002/aqc.525.

Sayre, R.G., Wright, D.J., Breyer, S.P., Butler, K.A., Van Graafeiland, K., Costello, M.J., Harris, P.T., Goodin, K.L., Guinotte, J.M., Basher, Z., Kavanaugh, M.T., Halpin, P.N., Monaco, M.E., Cressie, N., Aniello, P., Frye, C.E., Stephens, D. (2017): A three- dimensional mapping of the ocean based on environmental data. Oceanography, 30, 90–103, https://doi.org/10.5670/oceanog.2017.116.

Schwarzkopf, F.U., Biastoch, A., Böning, C.W., Chanut, J., Durgadoo, J.V., Getzlaff, K., Harlaß, J., Rieck, J.K., Roth, C., Scheinert, M.M., Schubert, R. (2019): The INALT family – a set of high-resolution nests for the

Agulhas Current system within global NEMO ocean/sea-ice configurations. Geoscientific Model Development, 12, 3329–3355, https://doi.org/10.5194/gmd-12-3329-2019.

Scrucca, L., and Raftery A.E. (2014): clustvarsel: A Package Implementing Variable Selection for Model-based Clustering in R. Journal of Statistical Software, 84, 1, https://www.jstatsoft.org/article/view/v084i01.

Scrucca, L., Fop, M., Murphy, T.B., Raftery, A.E. (2016): mclust 5: clustering, classification and density estimation using Gaussian finite mixture models. The R Journal, 8, 289-317, https://pubmed.ncbi.nlm.nih.gov/27818791/.

Semper, S., Pickart, R.S., Våge, K. (2020): The Iceland-Faroe Slope Jet: a conduit for dense water toward the Faroe Bank Channel overflow. Nature Communications, 11, 5390, https://doi.org/10.1038/s41467-020-19049-5.

Snelgrove, P.V.R. (1999): Getting to the Bottom of Marine Biodiversity: Sedimentary Habitats. BioScience, 49, 129-138, https://doi.org/10.2307/1313538.

Snelgrove, P.V.R (2010): Discoveries of the Census of Marine Life - Making Ocean Life Count. Cambridge University Press, Cambridge, United Kingdom.

Straume, E.O., Gaina, C., Medvedev, S., Hochmuth, K., Gohl, K., Whittaker, J.M., Abdul Fattah, R., Doornenbal, J.C., Hopper, J.R. (2019): GlobSed: Updated total sediment thickness in the world's oceans. Geochemistry, Geophysics, Geosystems, 20, 1756– 1772, https://doi.org/10.1029/2018GC008115.

Sonnewald, M., Dutkiewicz, S., Hill, C., Forget, G. (2020): Elucidating ecological complexity: Unsupervised learning determines global marine eco-provinces. Science Advances, 6, 22, https://advances.sciencemag.org/content/6/22/eaay4740.full.

Speer, K.G. and Zenk, W. (1993): The flow of Antarctic Bottom Water into the Brazil Basin. Journal of Physical Oceanography, 23, 2667 – 2682, https://doi.org/10.1175/1520-0485(1993)023<2667:TFOABW>2.0.CO;2.

Tozer, B., Sandwell, D.T., Smith, W.H.F., Olson, C., Beale, J.R., Wessel, P. (2019a). Global bathymetry and topography at 15 arc sec: SRTM15+. Open Topography. URL: https://doi.org/10.5069/G92R3PT9, Accessed in May 2021.

Tozer, B., Sandwell, D.T., Smith, W.H.F., Olson, C., Beale, J.R., Wessel, P. (2019b): Global bathymetry and topography at 15 arc sec: SRTM15+. Earth and Space Science, 6, 1847–1864, https://doi.org/10.1029/2019EA000658.

UNESCO (2009): Global Open Oceans and Deep Seabed (GOODS) – Biogeographic Classification. UNESCO-IOC (IOC Technical Series 84), Paris, France.

Van Rossum, G. and Drake, F.L. (2009): Python 3 Reference Manual. Createspace Independent Pub, Scotts Valley, California, USA.

Våge, K., Pickart, R.S., Spall, M.A., Valdimarsson, H., Jónsson, S., Torres, D.J., Østerhus, S., Eldevik, T. (2011): Significant role of the North Icelandic Jet in the formation of Denmark Strait overflow water. Nature Geoscience, 4, 723–727, https://doi.org/10.1038/ngeo1234.

Vasquez, M., Mata Chacón, D., Tempera, F., O'Keeffe, E., Galparsoro, I., Sanz Alonso, J.L., Gonçalves, J.M.S., Bentes, Amorim, L. P., Henriques, V., McGrath, F., Monteiro, P., Mendes, B., Freitas, R., Martins, R., Populus, J. (2015): Broad-scale mapping of seafloor habitats in the north-east Atlantic using existing

environmental data. Journal of Sea Research, 100, 120-132, https://doi.org/10.1016/j.seares.2014.09.011.

Verfaillie, E., Degraer, S., Schelfaut, K., Willems, W., Van Lancker V.A. (2009): A Protocol for classifying ecologically relevant marine zones, a statistical approach. Estuarine, Coastal and Shelf Science, 83, 175–185, https://doi.org/10.1016/j.ecss.2009.03.003Get rights and content.

Visalli, M.E., Best, B.D., Cabral, R.B., Cheung, W.W.L., Clark, N.A., Garilao, C., Kaschner, K., Kesner-Reyes, K., Lam, V.W.Y., Maxwell, S.M., Mayorga, J., Moeller, H.V., Morgan, L., Ortuño Crespo, G., Pinsky, M.L., White, T.D., McCauley, D.J. (2020): Data-driven approach for highlighting priority areas for protection in marine areas beyond national jurisdiction. Marine Policy, 122, 103927, https://doi.org/10.1016/j.marpol.2020.103927.

Watling, L., Guinotte, J., Clark, M.R., Smith, C.R. (2013): A proposed biogeography of the deep ocean floor. Progress in Oceanography, 111, 91-112, https://doi.org/10.1016/j.pocean.2012.11.003.

Weiss, A. (2001): Topographic Position and Landforms Analysis. The Nature Conservancy, URL: http://www.jennessent.com/downloads/tpi-poster-tnc_18x22.pdf, Accessed in May 2021.

Wessel, P., Luis, J.F., Uieda, L., Scharroo, R., Wobbe, F., Smith, W.H.F., Tian, D. (2019): The Generic Mapping Tools version 6. Geochemistry, Geophysics, Geosystems, 20, 5556–5564. https://doi.org/10.1029/2019GC008515.

Wickham, H. (2016). ggplot2: Elegant Graphics for Data Analysis. Springer-Verlag, New York, USA.

Yesson, C., Clark, M.R., Taylor, M., Rogers, A.D. (2011a): Lists of seamounts and knolls in different formats. PANGAEA, URL: https://doi.org/10.1594/PANGAEA.757564, Supplement to: Yesson, C., Clark, M.R., Taylor, M., Rogers, A.D. (2011): The global distribution of seamounts based on 30-second bathymetry data. Deep Sea Research Part I: Oceanographic Research Papers, 58, 442-453, https://doi.org/10.1016/j.dsr.2011.02.004.

Yesson, C., Clark, M.R., Taylor, M., Rogers, A.D. (2011b): The global distribution of seamounts based on 30 arc seconds bathymetry data. Deep Sea Research Part I: Oceanographic Research Papers, 58, 442-453, https://doi.org/10.1016/j.dsr.2011.02.004.

Zeng, C., Rowden, A.A., Clark, M.R., Gardner, J.P.A. (2020): Species-specific genetic variation in response to deep-sea environmental variation amongst Vulnerable Marine Ecosystem indicator taxa. Scientific Reports, 10, 2844, https://doi.org/10.1038/s41598-020-59210-0.

Zeppilli, D., Pusceddu, A., Trincardi, F., Danovaro, R. (2016): Seafloor heterogeneity influences the biodiversity–ecosystem functioning relationships in the deep sea. Scientific Reports, 6, 26352, https://doi.org/10.1038/srep26352.

Appendix

Table 2: Summary Statistics of input variables

	O2	O2_SV	Sal	Sal_SV	Vel	Vel_SV	Temp	Temp_SV	Phyc	Phyc_SV	Depth	TRI	TPI	Slope	POC	SedThick
Min. :	0	0	0,01208	0	0,0000002	0,0000002	-1,8705	0	0	0	-8399	0	-2192	0	0,04456	0
1st Qu.:	221,3	6,105	34,71939	0,001526	0,0083402	0,0134352	0,6176	0,01742	0,01356	0,000351	-4824	131,5	-44,258	0,1918	1,40309	123
Median :	241,8	6,58	34,88533	0,003901	0,0157552	0,0223072	1,865	0,04118	0,01367	0,000358	-3976	316,8	-1,439	0,4762	2,24798	500
Mean :	242,1	7,338	34,81067	0,030581	0,0292069	0,0299032	2,5	0,20937	0,12818	0,058779	-3553	488	-0,67	0,8141	8,38344	1319
3rd Qu.:	261,7	7,252	34,91496	0,013054	0,0331452	0,0374932	2,4278	0,10311	0,01402	0,000387	-2725	638	33,252	1,0255	4,01226	1513
Max. :	359,3	105,088	38,53865	14,637185	1,4602322	0,5535792	30,3565	22,3883	23,84801	23,589828	0	9510,9	3186,442	17,6801	220,05	18171

Table 3: Summary Statistics of input variable per SBA

Mean																
SBAs	Depth	Slope	TRI	TPI	SedThick	POC	O2	O2_SV	Vel	Vel_SV	Sal	Sal_SV	Temp	Temp_SV	Phyc	Phyc_SV
1	-2543,718	0,597	321,198	-4,633	2097	5,562	288,224	7,671	0,024	0,021	34,928	0,006	1,145	0,057	0,016	0,001
2	-3287,079	1,746	1041,221	22,203	2143	3,143	230,169	6,593	0,034	0,033	34,868	0,014	2,256	0,097	0,014	0,000
3	-4724,678	0,272	149,936	-3,109	1427	2,569	232,969	6,302	0,033	0,043	34,794	0,005	1,019	0,047	0,014	0,000
4	-789,599	1,071	523,512	12,926	3399	24,791	234,892	8,156	0,068	0,034	34,938	0,060	5,803	0,369	0,081	0,027
5	-3692,313	0,780	452,923	-11,141	452	2,119	238,523	6,596	0,027	0,027	34,780	0,003	0,913	0,044	0,014	0,000
6	-4893,159	0,878	592,156	-5,773	235	1,557	245,532	6,472	0,010	0,016	34,859	0,002	1,567	0,015	0,014	0,000
7	-4970,350	0,295	173,709	-3,663	1378	2,187	270,186	7,092	0,049	0,060	34,894	0,001	1,794	0,016	0,014	0,000
8	-4105,158	0,933	596,294	-9,606	165	1,819	233,287	6,315	0,014	0,022	34,817	0,009	1,366	0,072	0,014	0,000
9	-85,330	0,109	67,121	1,274	2873	62,810	246,282	16,078	0,047	0,037	34,296	0,305	12,095	2,024	1,666	0,855
Median																
1	-2601,166	0,395	217,161	-1,681	1254	5,562	285,616	7,720	0,014	0,018	34,919	0,004	1,892	0,043	0,015	0,000
2	-3275,275	1,071	695,457	-2,348	1006	3,143	230,475	6,483	0,020	0,026	34,899	0,007	2,256	0,060	0,014	0,000
3	-4824,048	0,209	126,323	-1,261	1036	2,569	233,306	6,239	0,022	0,034	34,780	0,003	0,967	0,030	0,014	0,000

4	-590,000	0,513	264,463	1,070	2496	24,791	252,163	7,818	0,035	0,026	34,926	0,038	4,394	0,265	0,039	0,007
5	-3688,568	0,587	381,889	-6,459	400	2,119	227,934	6,593	0,019	0,022	34,704	0,002	0,376	0,037	0,014	0,000
6	-4944,198	0,712	519,609	-5,924	120	1,557	245,157	6,436	0,009	0,014	34,887	0,001	1,907	0,014	0,014	0,000
7	-4996,718	0,202	132,453	-1,578	999	2,187	269,195	7,024	0,041	0,054	34,895	0,001	1,805	0,015	0,014	0,000
8	-4062,018	0,753	517,559	-8,644	102	1,819	234,728	6,303	0,011	0,019	34,821	0,007	1,428	0,059	0,014	0,000
9	-76,537	0,056	37,450	0,129	1946	62,810	259,248	12,357	0,027	0,027	34,625	0,140	9,990	0,843	0,976	0,550
1st Quartile																
1	-3063,001	0,193	111,720	-26,933	500	3,058	275,467	7,320	0,007	0,011	34,915	0,002	-0,855	0,015	0,014	0,000
2	-4090,029	0,439	291,597	-89,352	279	1,639	216,050	5,912	0,010	0,015	34,765	0,002	1,213	0,024	0,014	0,000
3	-5135,580	0,113	70,104	-16,587	603	1,738	219,951	5,796	0,011	0,021	34,676	0,001	-0,090	0,016	0,013	0,000
4	-1195,306	0,183	103,148	-20,617	900	8,619	194,098	6,327	0,015	0,015	34,661	0,020	3,080	0,134	0,018	0,001
5	-4135,346	0,302	225,911	-65,321	203	0,940	215,838	5,936	0,010	0,013	34,676	0,001	-0,136	0,023	0,014	0,000
6	-5347,471	0,367	315,697	-89,325	101	1,014	239,250	6,257	0,005	0,009	34,874	0,001	1,682	0,008	0,014	0,000
7	-5268,814	0,101	74,947	-19,388	735	1,580	266,961	6,910	0,027	0,035	34,890	0,001	1,763	0,009	0,014	0,000
8	-4640,634	0,420	337,896	-91,900	93	1,184	219,031	5,945	0,007	0,013	34,731	0,004	0,573	0,036	0,014	0,000
9	-119,606	0,027	18,977	-4,384	905	37,111	204,754	8,569	0,014	0,016	33,614	0,068	6,701	0,436	0,520	0,181
3rd Quartile																
1	-2064,048	0,772	420,208	19,127	2940	6,370	301,183	7,946	0,028	0,028	34,938	0,008	2,806	0,082	0,018	0,001
2	-2443,081	2,379	1555,503	86,627	3148	3,711	246,164	7,061	0,041	0,043	34,965	0,019	3,444	0,132	0,014	0,000
3	-4385,298	0,371	206,075	11,193	1972	3,238	244,281	6,687	0,044	0,056	34,890	0,008	1,907	0,061	0,014	0,000
4	-299,751	1,322	643,428	28,632	5107	36,107	282,034	9,661	0,081	0,043	35,114	0,077	7,519	0,496	0,099	0,034
5	-3236,000	1,052	603,579	42,986	589	3,514	269,866	7,245	0,037	0,036	34,914	0,003	2,074	0,058	0,014	0,000
6	-4473,223	1,210	795,157	73,673	287	1,981	249,986	6,658	0,013	0,021	34,896	0,002	1,991	0,021	0,014	0,000
7	-4720,001	0,393	230,157	13,503	1824	2,777	270,761	7,211	0,066	0,080	34,897	0,002	1,829	0,022	0,014	0,000
8	-3563,805	1,258	779,382	74,620	201	2,250	245,522	6,691	0,018	0,028	34,896	0,012	2,099	0,095	0,014	0,000
9	-39,947	0,123	76,574	5,522	3983	82,453	278,126	20,577	0,056	0,048	35,398	0,301	18,364	2,187	1,978	1,032

Table 4: Comparison of existing similar analyses to iAtlantic SBAs - Cluster Description

iA SBA Description	Global Seascapes (Harris et al., 2009)	GOODS (UNESCO, 2009/Watling, 2013)	EMU (Sayre et al., 2019)
SBA I: Oxic, POC flux influenced, mostly flat with regionally thick sediment cover sedimented, current influenced regions with low seasonal change	**Seascape 7**: 'Abyssal, volcanic ridges and high, central rift zone, ridge flanks, microcontinents, cold' **Seascape 4**: 'Lower Bathyal, continental slope, steep, high [primary production], very thick sediment, warm'	**LBP[2]2**: Northern North Atlantic, from the Iceland-Faroe Ridge in the north south along the Reykjanes Ridge, over the Newfoundland Seamounts and following the Western Boundary Undercurrent southward along the eastern slope of North America to off Cape Hatteras;	**EMU 29**: Deep, Very Cold, Normal Salinity, Moderate Oxygen, Medium Nitrate, Low Phosphate, Low Silicate;
SBA II: MAR spreading centre including abyssal ridges, trenches and continental slopes	**Seascape 2**: 'Lower bathyal, deep shelf (submerged), marginal plateaus, very high [dissolved oxygen], high [primary productivity], thick sediment, warm', **Seascape 4**: 'Lower Bathyal, continental slope, steep, high [primary production], very thick sediment, warm', **Seascape 5**: 'Lower Bathyal, island arcs, steep, high [dissolved oxygen]' **Seascape 9**: 'Abyssal (hadal) trenched, controlled by fracture zones, deep water trenched, large arched uplifted structures, low [primary production], thin sediment, cold'	**LBP4**: North Atlantic, extends southward along the Mid-Atlantic Ridge from the Reykjanes Ridge to approximately the equator, and along the eastern and western margins of the North Atlantic Ocean including the Caribbean Sea and Gulf of Mexico; **LBP13**: South Atlantic, encompassing all of the South Atlantic from about the Equator to the Antarctic Convergence;	**EMU 13**: Deep, Very Cold, Normal Salinity, Low Oxygen, High Nitrate, Medium Phosphate, High Silicate (patchy); **EMU 14:** Deep, Very Cold, Normal Salinity, Moderate Oxygen, High Nitrate, Low Phosphate, High Silicate (South Atlantic); **EMU 36**: Deep, Very Cold, Normal Salinity, Moderate Oxygen, Medium Nitrate, Low Phosphate, Low Silicate; **EMU 37**: Deep, Very Cold, Normal Salinity, Moderate Oxygen, High Nitrate, Low Phosphate, Medium Silicate (South to Central Atlantic);
SBA III: Deep, cold, fresh & oxygen depleted abyssal plain with increased bottom current velocity	**Seascape 10**: 'Abyssal, plains with slightly undulating seafloor, flat abyssal plains, continental rise, very flat, high [dissolved oxygen], low [primary production], very cold '	**AP[3]2**: North Atlantic; including all areas north of the equator under the influence of North Atlantic Deep water; **AP3**: Brazil Basin; extending south from the hump of Brazil bordering the Romanche Fracture to Sao Paulo; **AP4**: Angola and Sierra Leone Basins; to the west of the Congo Fan in the North and limited by the Walvis Ridge to the SE and including the Namibia abyssal plain; **AP5**: Argentine Basin; from Rio de la Plata to the Falkland Escarpment in the south; **AP6**: East Antarctic Indian, which includes the areas where very cold bottom water flows into Namibia, Cape, Agulhas, Natal, and Crozet and South Indian Basins;	**EMU 14:** Deep, Very Cold, Normal Salinity, Moderate Oxygen, High Nitrate, Low Phosphate, High Silicate (South Atlantic); **EMU 36**: Deep, Very Cold, Normal Salinity, Moderate Oxygen, Medium Nitrate, Low Phosphate, Low Silicate; **EMU 37**: Deep, Very Cold, Normal Salinity, Moderate Oxygen, High Nitrate, Low Phosphate, Medium Silicate (South to Central Atlantic);
SBA IV: Shallow, warm, nutrient-rich and saline deeper shelf zones with thick sediment cover, strong currents and strong local and seasonal changes	**Seascape 2**: 'Lower bathyal, deep shelf (submerged), marginal plateaus, very high [dissolved oxygen], high [primary productivity], thick sediment, warm' **Seascape 5**: 'Lower Bathyal, island arcs, steep, high [dissolved oxygen]'	**LBP2**: Northern North Atlantic, from the Iceland-Faroe Ridge in the north south along the Reykjanes Ridge, over the Newfoundland Seamounts and following the Western Boundary Undercurrent southward along the eastern slope of North America to off Cape Hatteras; **LBP13**: South Atlantic, encompassing all of the South Atlantic from about the Equator to the Antarctic Convergence;	**EMU 10:** Mesopelagic, Cold, Euhaline, Severely Hypoxic, High Nitrate, Low Phosphate, Low Silicate Common (Central Atlantic); **EMU 11**: Epipelagic, Moderate to Cool, Euhaline, Oxic, Low Nitrate, Low Phosphate, Low Silicate (North & South Atlantic); **EMU 21**: Shallow, Warm, Normal Salinity, Moderate Oxygen, Low Nitrate, Low Phosphate, Low Silicate (Central Atlantic);

[2] LBP: Lower Bathyal Province, as in UNESCO, 2009

[3] AP: Abyssal Province, as in UNESCO, 2009

SBA V: Small & regional, cold and fresh deep water influenced areas in North & South Atlantic at medium depth, with locally increased currents and current seasonal change	**Seascape 10**: 'Abyssal, plains with slightly undulating seafloor, flat abyssal plains, continental rise, very flat, high [dissolved oxygen], low [primary production], very cold	North-Western part of **AP2**: North Atlantic; including all areas north of the equator under the influence of North Atlantic Deep water; **AP6**: East Antarctic Indian, which includes the areas where very cold bottom water flows into Namibia, Cape, Agulhas, Natal, and Crozet and South Indian Basins; Fractions of **LBP2**: Northern North Atlantic, from the Iceland-Faroe Ridge in the north south along the Reykjanes Ridge, over the Newfoundland Seamounts and following the Western Boundary Undercurrent southward along the eastern slope of North America to off Cape Hatteras; in North and South Atlantic: **LBP13**: South Atlantic, encompassing all of the South Atlantic from about the Equator to the Antarctic Convergence;	**EMU 29**: Deep, Very Cold, Normal Salinity, Moderate Oxygen, Medium Nitrate, Low Phosphate, Low Silicate (North Atlantic); **EMU 36**: Deep, Very Cold, Normal Salinity, Moderate Oxygen, Medium Nitrate, Low Phosphate, Low Silicate; **EMU 37**: Deep, Very Cold, Normal Salinity, Moderate Oxygen, High Nitrate, Low Phosphate, Medium Silicate (South to Central Atlantic)
SBA VI: Central deep Atlantic cool, nutrient-depleted area with very weak currents, covering some abyssal elevations and sinks	**Seascape 10:** 'Abyssal, plains with slightly undulating seafloor, flat abyssal plains, continental rise, very flat, high [dissolved oxygen], low [primary production], very cold ' **Seascape 6**: 'Lower Bathyal (Abyssal-Hadal), deep water trenches, island arcs, tranches controlled by fracture zones, volcanic ridges and plateaus, very steep' **Seascape 9**: 'Abyssal (hadal) trenched, controlled by fracture zones, deep water trenched, large arched uplifted structures, low [primary production], thin sediment, cold'	**AP2**: North Atlantic; including all areas north of the equator under the influence of North Atlantic Deep water; South – Eastern Atlantic: **AP4**: Angola and Sierra Leone Basins; to the west of the Congo Fan in the North and limited by the Walvis Ridge to the SE and including the Namibia abyssal plain;	**EMU 36**: Deep, Very Cold, Normal Salinity, Moderate Oxygen, Medium Nitrate, Low Phosphate, Low Silicate; **EMU 37**: Deep, Very Cold, Normal Salinity, Moderate Oxygen, High Nitrate, Low Phosphate, Medium Silicate (South to Central Atlantic)
SBA VII: Small & regional, deep, flat, sedimented oxic region with strong currents and high seasonal current change	**Seascape 10**: 'Abyssal, plains with slightly undulating seafloor, flat abyssal plains, continental rise, very flat, high [dissolved oxygen], low [primary production], very cold '	North American basin: **AP2**: North Atlantic; including all areas north of the equator under the influence of North Atlantic Deep water;	**EMU 36**: Deep, Very Cold, Normal Salinity, Moderate Oxygen, Medium Nitrate, Low Phosphate, Low Silicate (Central Atlantic);
SBA VIII: Wider region around MAR covering new seafloor, faults and fracture zones, with extremely low sediment cover, no currents, very low oxygen and temperature	**Seascape 7**: 'Abyssal, volcanic ridges and high, central rift zone, ridge flanks, microcontinents, cold' and **Seascape 5**: 'Lower Bathyal, island arcs, steep, high [dissolved oxygen]' and **Seascape 9**: 'Abyssal (hadal) trenched, controlled by fracture zones, deep water trenched, large arched uplifted structures, low [primary production], thin sediment, cold'	South of Argentina: **AP7**: West Antarctic, includes the Amundsen and Bellinghausen abyssal Plains in the region from the Ross Sea to the Antarctic Peninsula and north to the Antarctic-Pacific Ridge and the Southeast Pacific Basin; South & Central Atlantic: **AP2**: North Atlantic; including all areas north of the equator under the influence of North Atlantic Deep water; **AP4**: Angola and Sierra Leone Basins; to the west of the Congo Fan in the North and limited by the Walvis Ridge to the SE and including the Namibia abyssal plain; Central/North Atlantic: **LBP4**: North Atlantic, extends southward along the Mid-Atlantic Ridge from the Reykjanes Ridge to approximately the equator, and along the eastern and western margins of the North Atlantic Ocean	**EMU 36**: Deep, Very Cold, Normal Salinity, Moderate Oxygen, Medium Nitrate, Low Phosphate, Low Silicate (Central Atlantic); **EMU 37**: Deep, Very Cold, Normal Salinity, Moderate Oxygen, High Nitrate, Low Phosphate, Medium Silicate (South to Central Atlantic)

		including the Caribbean Sea and Gulf of Mexico;	
SBA IX: Oxic, POC flux influenced, mostly flat with regionally thick sediment cover sedimented, current influenced regions with low seasonal change	excluded	excluded	**EMU 11**: Shallow, Cool, Normal Salinity, Moderate Oxygen, Low Nitrate, Low Phosphate, Low Silicate (South West and North East Atlantic); **EMU 21**: Shallow, Warm, Normal Salinity, Moderate Oxygen, Low Nitrate, Low Phosphate, Low Silicate (wider Central Atlantic); **EMU 24**: Epipelagic, Warm to Very Warm, Euhaline, Oxic, Low Nitrate, Low Phosphate, Low Silicate (Central Atlantic)

Table 5: Comparison of existing similar analyses to iAtlantic SBAs - Methods

	iA SBAs	Global Seascapes (Harris et al., 2008)	GOODS (UNESCO, 2009/Watling, 2013)	EMU (Sayre et al., 2019)
No. of clusters (in Atlantic basin)	9	8	12 [4 (lower bathyal: BY1,2,4,13); 5 (abyssal: AB2-6); 3 (hadal: HD8-10)]	8
Classification method	Unsupervised (mclust)	Unsupervised (ER-Mapper isoclass)	Hierarchical depth-dependant; Delphic (expert knowledge);	Unsupervised (KMeans)
Depth level	Benthic	Benthic	Pelagic; Benthic: upper & lower bathyal, abyssal, hadal;	Epipelagic, Mesopelagic, Benthopelagic, Abyssopelagic
Model data resolution [°]	1/12	1/10	-	1/4
Input data/Source:				
Depth	SRTM15+V2	ETOPO2	ETOPO2; GEBCO 2003	WOA depth intervals
Slope	v	v	-	-
TPI	v	-	-	-
TRI	v	-	-	-
POC	Lutz 2007	-	Yool 2007	-
Phytoplankton	CMEMS	-	-	-
Sediment	GLOBSED; Straume et al. 2019	NGDC; Divins 1998	NGDC; Divins 1998	-
Current Speed	CMEMS	-	-	-
Current Direction	-	-	-	-
Salinity	CMEMS	-	WOA	WOA
Temperature	CMEMS	WOA	WOA	WOA
Oxygen	CMEMS	WOA	WOA	WOA
Seasonality	CMEMS	-	-	-
Species	-	-	several	-

Else	-	Primary Production (SeaWIFs), Sediment types (Davies & Gorsline 1976)	Seamounts (Kitchiman & Lai 2004), Hydrthermal vents (InterRidge and Cindy VanDover), Plate boundaries (PLATES, University of Texas), SST (NASA); Primary Productivity (OregonState University), Cold Water Coral Reefs (UNEP-WCMC), Global Ocean Current systems and gyres	Nitrate, Phosphate, Silicate (WOA)

6. Document Information

EU Project N°	818123	Acronym	iAtlantic
Full Title	Integrated Assessment of Atlantic Marine Ecosystems in Space and Time		
Project website	www.iatlantic.eu		

Deliverable	N°	D2.1	Title	Basin-wide Atlantic marine landscape map
Work Package	N°	2	Title	Mapping deep Atlantic ecosystems

Date of delivery	Contractual	December 2020	Actual	September 2021
Dissemination level	X	PU Public, fully open, e.g. web		
		CO Confidential restricted under conditions set out in Model Grant Agreement		
		CI Classified, information as referred to in Commission Decision 2001/844/EC		

Authors (Partner(s))	GEOMAR, NOC, SGN, Research Vessel Sonne			
Responsible Authors	Names	• Mia Schumacher • Veerle Huvenne • Colin Devey • Pedro Martínez Arbizu • Arne Biastoch • Stefan Meinecke	Emails	• mschumacher@geomar.de • vaih@noc.ac.uk • cdevey@geomar.de • pmartinez@senckenberg.de • abiastoch@geomar.de • stefan.meinecke@email.de